IMPETUS

driving precision

Validation - Terminal Ballistics

Solver version: 8.1.603
Date: October 2, 2023

Introduction

This document presents validation tests on terminal ballistics.

Numerical models of experiments are created and evaluated against the experimental results. Experimental data is gathered from several scientific studies reported in literature. Key materials and projectiles used in the models are available as material objects on IMPETUS Market.

Version control

Most of the tests presented in this document are subjected to version control, meaning that the models are run and evaluated prior to release of a new solver. This document is updated in conjunction with new official releases of the software.

Overview of tests

Information regarding projectiles and target materials used in the different validation cases are presented in the Table below.

Article	**Type of projectile(s)**	**Material in target**
T. Børvik et al. (2009) (1)	Steel cylinders (conical nose)	AA5083-H116
J. K. Holmen et al. (2013)	7.62 mm APM2	AA6070
T. Børvik et al. (2011)	7.62 mm APM2	AA6082-T4
T. Børvik et al. (2009) (2)	7.62 mm APM2	Domex Protect 500, Hardox 400 Weldox 500E and Weldox 700E
S. J. Schraml (2012)	Tungsten cylinders (hemispherical nose)	RHA (Rolled Homogenous Armor)
J. P Riegel III and D. Davison (2016)	Tungsten cylinders	RHA
E. Lidén et al. (2007)	WHA (Wolfram Heavy Alloy) cylinders	SS2541-03
P. Weidemaier et al. (2004)	WHA cylinders	RHA
P. Lundberg (2004)	Steel cylinders	SiC (Silicon Carbide)
C. G. Fountzoulas et al. (2009)	WC (Wolfram Carbide) ball	SiC
L. H. Nguyen et al. (2016)	20 mm FSP (Fragment Simulating Projectile)	Dyneema HB26
K. Karthikeyan et al. (2013)	Steel ball	Dyneema HB26

C. G. Fountzoulas et al. (2009)

Simulation of Ballistic Impact of a Tungsten Carbide Sphere on a Confined Silicon Carbide Target

Silicon carbide (SiC-N) cylinders in titanium alloy (Ti-6Al-4V) cups impacted by tungsten carbide (WC) spheres at impact velocities in the range of 50 - 500 m/s are investigated in C. G. Fountzoulas et al. (2009) [1]. The SiC-N cylinders are manufactured by CERCOM, inc. A model of the experiments is created and the simulations are compared to cross-sectional images of the SiC-N cylinders post testing, gathered from the referenced literature.

The diameter and height of the SiC-N cylinders is 25.4 mm and the diameter of the WC spheres is 6.35 mm. The inner diameter of the titanium cups is 24.425 mm while the outer diameter is not stated. A wall thickness of 10.0 mm is assumed.

The material object of SiC-N is used for the silicone carbide. Material properties used for Ti-6Al-4V and WC are displayed in Table 2. Full models (w/o symmetry) are used in the simulations. A fine mesh is required to get crack patterns that resembles the ones seen in the experiments. An image of the model is presented in Figure 1.

Table 2: Material properties for the wolfram carbide and the titanium alloy. The titanium alloy is modeled as linear-elastic.

Material	**Density** $[kg/m^3]$	**Young's modulus** $[GPa]$	**Static yield strength** $[GPa]$
WC	14470	620	3.5
Ti-6Al-4V	4430	110	-

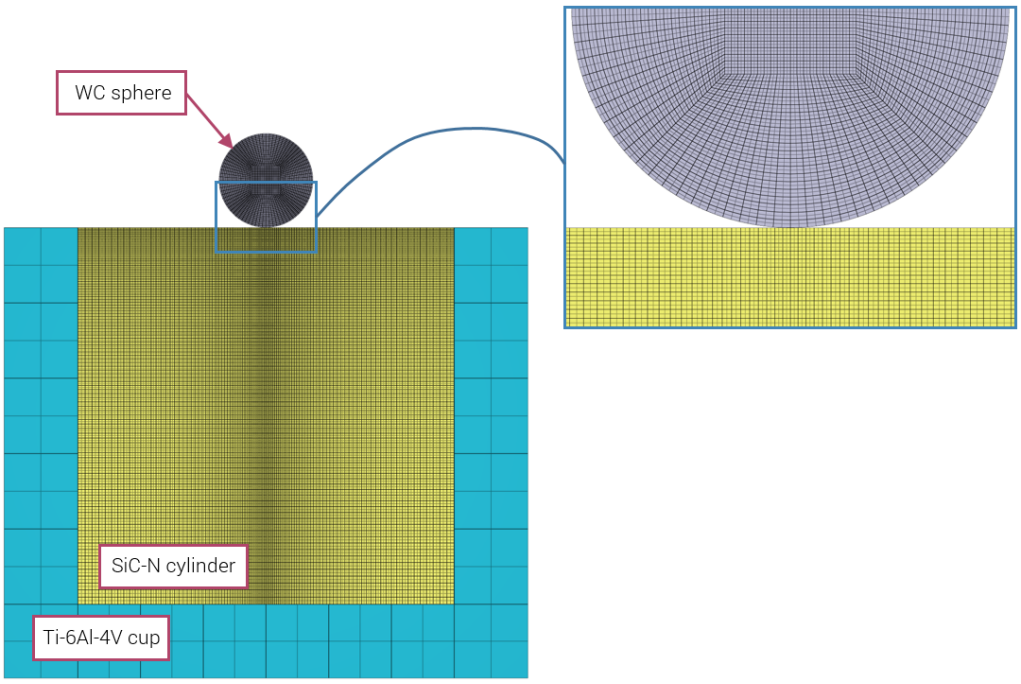

Figure 1: Cross-sectional side view of the model.

Impact velocities under consideration are 63, 161, 322 and 500 m/s. The final state of the simulations are compared to the cross-section cylinders from the experiment post testing in Figure 2 - 5.

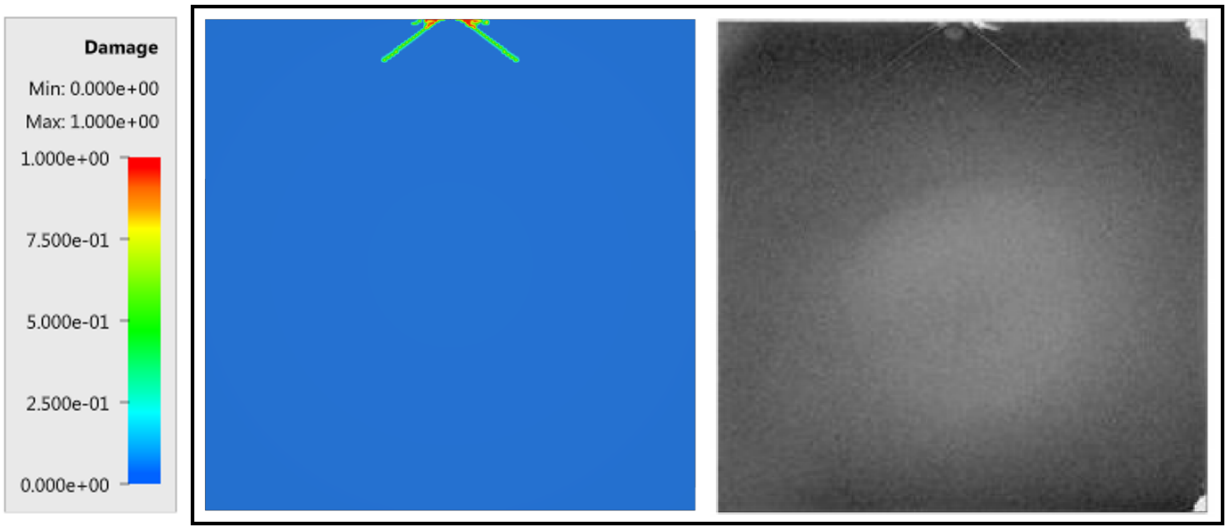

Figure 2: Comparison between simulation and experiment at impact velocity = 63 m/s.

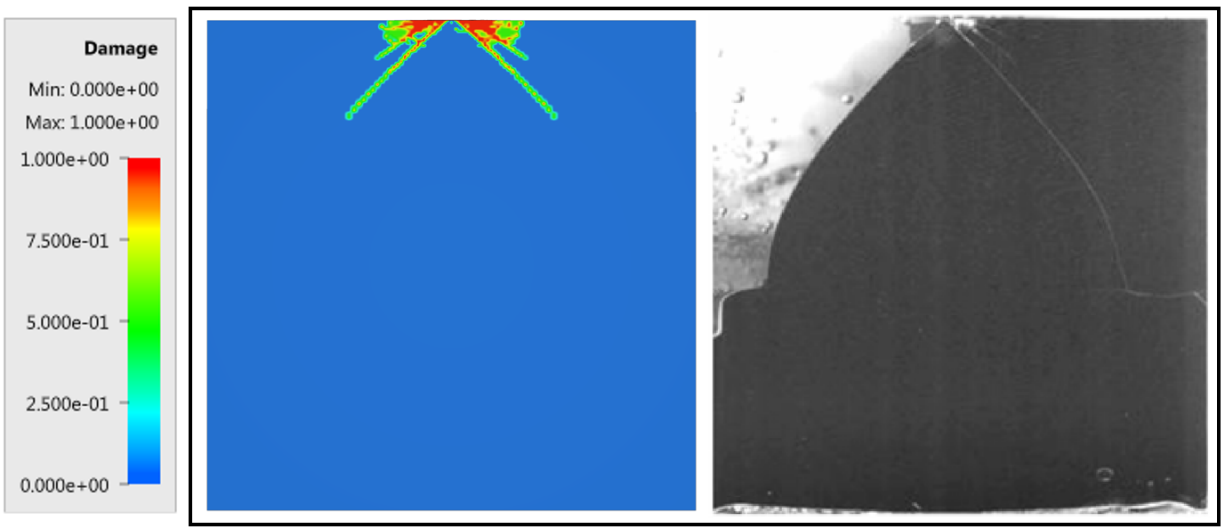

Figure 3: Comparison between simulation and experiment at impact velocity = 161 m/s.

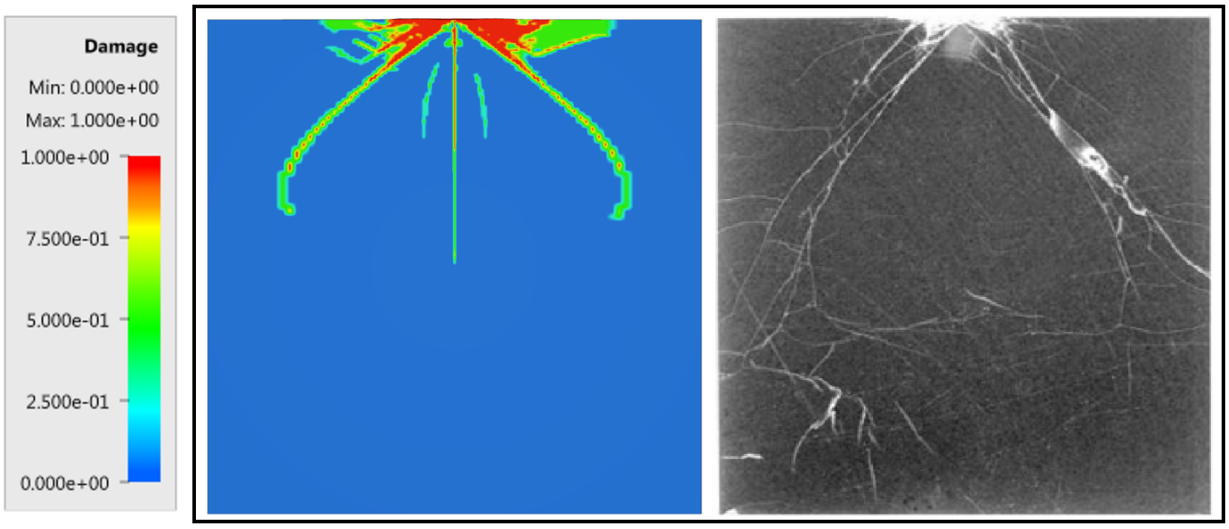

Figure 4: Comparison between simulation and experiment at impact velocity = 322 m/s.

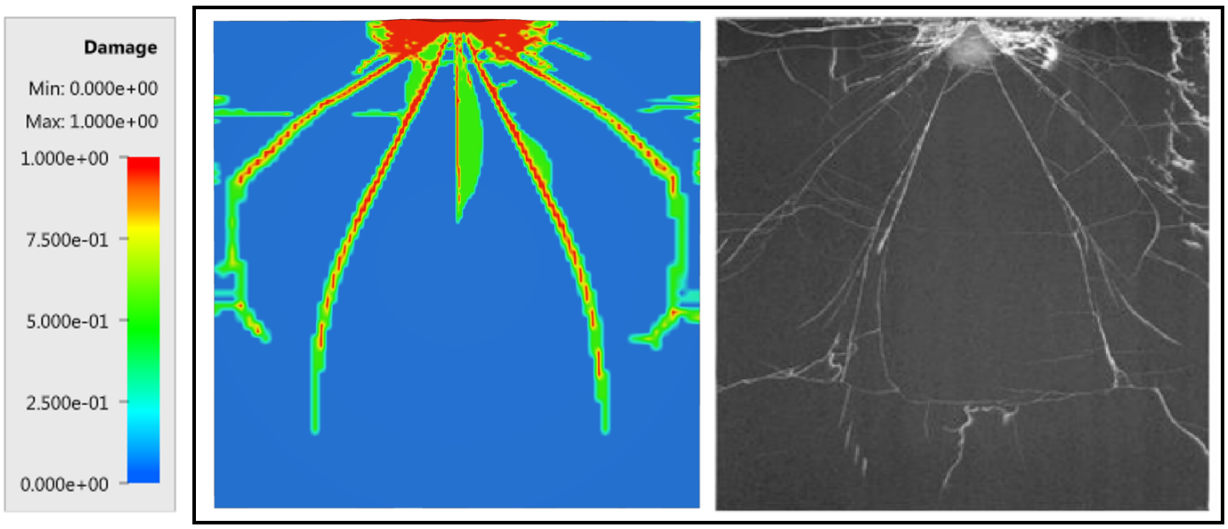

Figure 5: Comparison between simulation and experiment at impact velocity = 500 m/s.

The model with an initial velocity of 161 m/s is subjected to version control.

References

1 - C. G. Fountzoulas et al. - Simulation of Ballistic Impact of a Tungsten Carbide Sphere on a Confined Silicon Carbide Target, Army Research Laboratory, 2009.

Tests

This benchmark is associated with 1 tests.

E. Lidén et al. (2007)

Influence of Side-Impacting Dynamic Armour Components on Long Rod Projectiles

LRPs (Long Rod Projectiles) of WHA impacted by steel rods is investigated in E. Lidén (2007) [1]. Seven different configurations with varying rod velocities, location of impact along the projectile, number of impacting rods and spacing between rods are investigated, with details presented in Table 3 and Figure 6. The LRP velocity was 2000 m/s and the angle between the velocity vectors is 120 degrees in all configurations. The diameter of both projectile and rods is 2 mm. The projectile length is 60 mm while the length of the rods are assumed to be 30 mm.

Table 3: Penetration depths in experiments and simulations at different impact velocities.

Configuration	**Number of rods**	**Velocity, V_{rod}** $[m/s]$	**Distance, D_s** $[mm]$	**Distance, D_0** [mm]
1	1	200	-	2 (assumed)
2	1	600	-	5
3	1	200	-	30
4	1	600	-	29
5	3	200	3	1, 20 and 29
6	3	600	3	6, 15 and 24
7	3	600	6.75	1, 21 and 41

Figure 6: To the left: one steel rod is used in configuration 1-4. To the right: three steel rods are used in configuration 5-7.

Model settings:

- Third order hexahedrons are used exclusively.
- LRP modeled with 2000 elements and each rod with 3200 elements, gradually refined towards center, as visible in Figure 7.
- Rods consist of steel grade SS2531-03, modeled with *MAT_JC with parameters in accordance with Table 4.
- A deviatoric erosion strain of 3.0 (300%) is used to maintain a reasonable time step size.
- A friction coefficient of 0.025 (2.5%) is assumed.

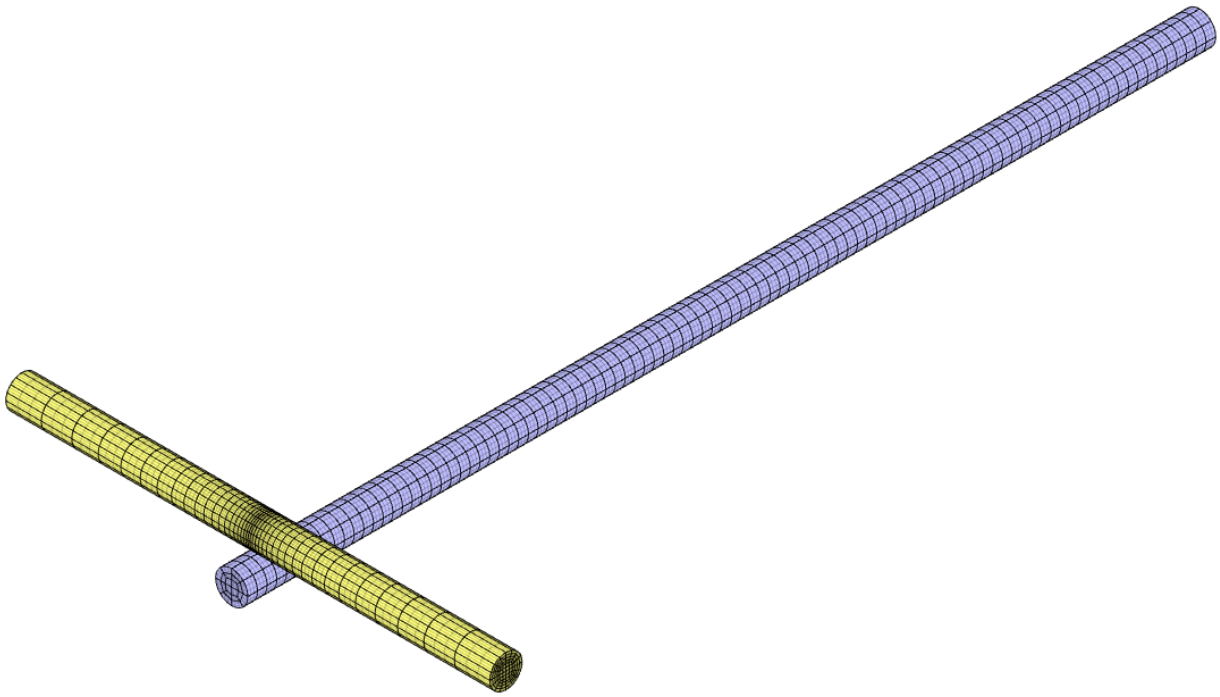

Figure 7: Mesh of projectile and rod.

Table 4: *MAT_JC parameters for steel grade SS2541-03

A $[MPa]$	**B** $[MPa]$	**n** $[-]$	**C** $[-]$	**m** $[m]$	$\mathbf{T_{melt}}$ $[K]$	ε_0 $[1/s]$
750	1150	0.49	0.014	1	1700	1

Simulations are compared to images from the experiments at different times after impact in Figure 8 .

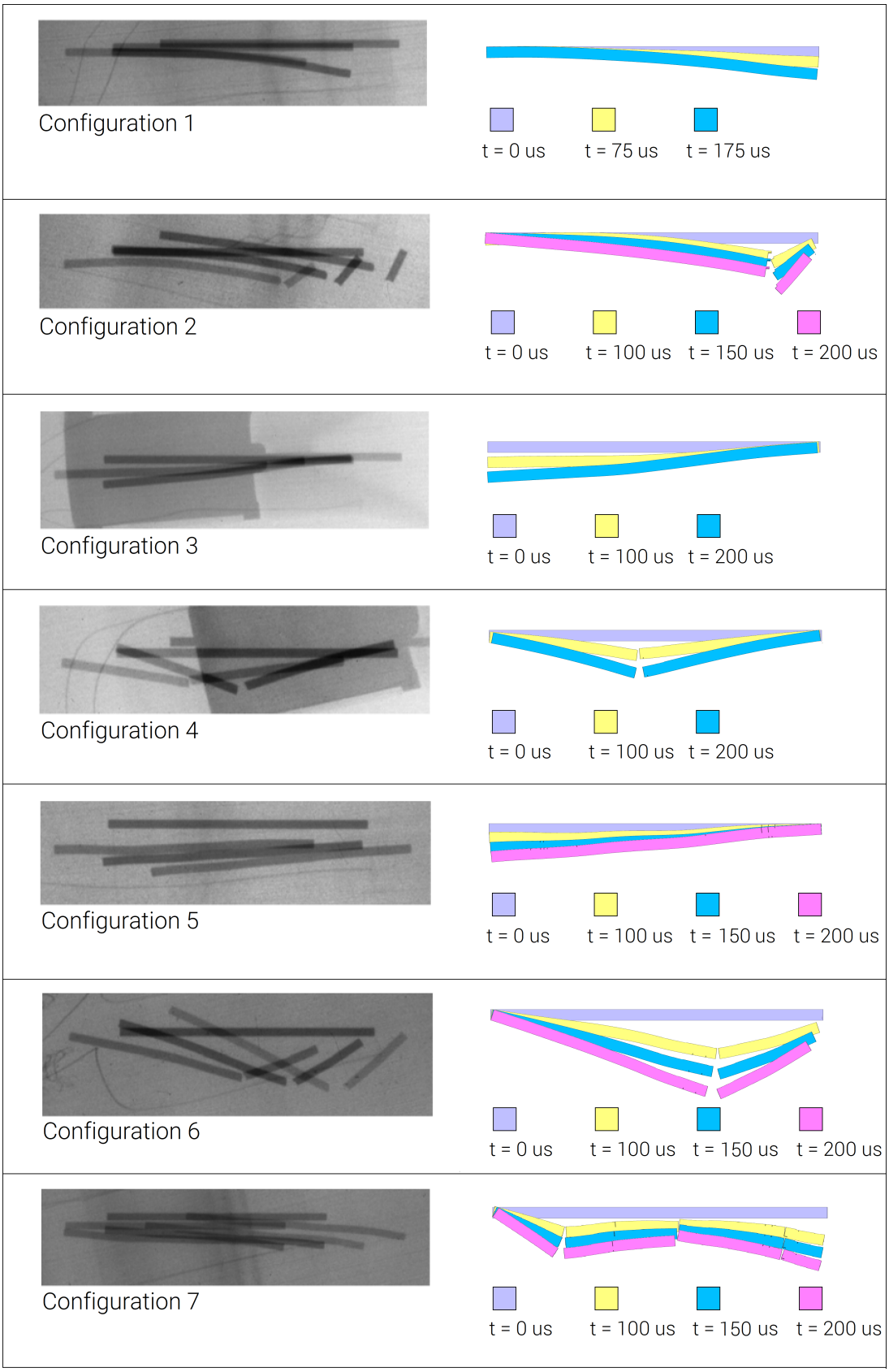

Figure 8: Simulations compared to images from the experiments at different times after impact.

The models of configuration 1 and 2 are subjected to version control.

References

1 - E. Lidén, O. Andersson, A. Tjernberg, Influence of Side-Impacting Dynamic Armour Components on Long Rod Projectiles, International Symposium on Ballistics, Volume 23, 2007, Pages 1099-1106.

Tests

This benchmark is associated with 2 tests.

J. K. Holmen et al. (2013)

Effects of heat treatment on the ballistic properties of AA6070 aluminium alloy

Perforation experiments with 7.62 mm APM2 projectiles on plates of AA6070 are presented in J. K. Holmen et al. (2013) [1]. A numerical model of the experiments is created to assess the calibrations of AA6070 available as Material objects.

AA6070 plates with dimensions 300 x 300 x 20 mm are fixed at two opposite edges while the other two edges are unconstrained. The target is modeled with the calibrations of AA6070. The 7.62 mm APM2 projectile core is modeled as rigid, while models of brass and lead, which are used in the jacket and tip, are modeled as described in T. Børvik et al. (2009) [2].

Model settings:

- Third order hexahedrons are used exclusively.
- Cubic elements with side length of approximately 1.0 mm are used in the impact zone.
- Quarter symmetry utilized as visible in Figure 9.
- A deviatoric erosion strain of 3.0 (300%) is used to maintain a reasonable time step size.
- Two friction coefficients are investigated: 0.05 (5%) and 0.1 (10%).

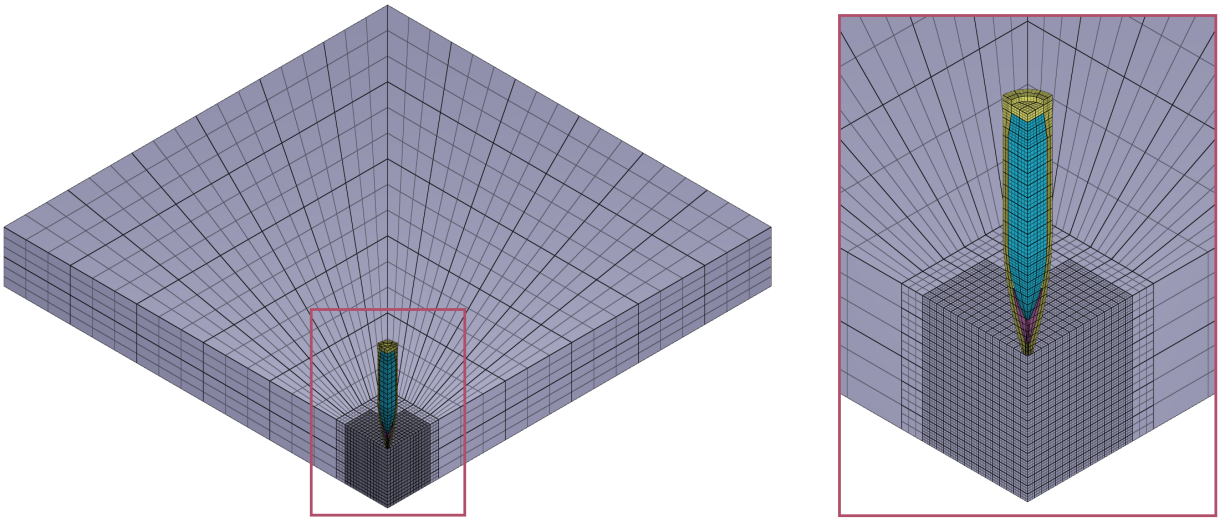

Figure 9: Quarter symmetry model of target plate and the 7.62 mm APM2 projectile. The target plate mesh is refined in the impact zone.

Regarding failure mechanism, the following is observed in the experiments:

- Ductile hole growth is the predominant failure mechanism for lower impact velocities while the degree of fragmentation is increased at higher velocities.
- Most fragmentation is seen for Temper T6 while no fragmentation is observed for temper O.
- High impact velocities generate fragmentation of the rear side of the plate while fragmentation of the front side is seen for lower velocities.

Residual velocities from the models are compared to Recht-Ipson curves based on residual velocities found from the experiments. The results are presented in Table 5, Table 6 and Figure 10 - 13. Cross-sectional views of the target plates from simulations are compared to photos from the experiments in Figure 14 - 18.

Table 5: Residual velocities from experiment, $v_{r,exp}$, and simulations, $v_{r,sim}$, at different impact velocities, v_0. Simulation results are with a friction coefficient of 0.05 (5%).

Templer	$\mathbf{v_0}$ $[m/s]$	$\mathbf{v_{r,exp}}$ $[m/s]$	$\mathbf{v_{r,sim}}$ $[m/s]$	**Error** [%]
O	348	0	140	-
	486	335	361	7.8
	624	511	523	2.3
	762	671	672	0.1
	900	830	839	1.1
T4	506	0	100	-
	605	341	377	10.6
	703	498	542	8.8
	802	632	671	6.2
	900	753	787	4.5
T6	562	0	229	-
	646	354	394	11.3
	731	504	531	5.4
	815	627	653	4.1
	900	740	760	2.7
T7	529	0	214	-
	622	360	393	9.2
	715	515	541	5.0
	807	643	668	3.9
	900	761	779	2.4

Table 6: Residual velocities from experiment, $v_{r,exp}$, and simulations, $v_{r,sim}$, at different impact velocities, v_0. Simulation results are with a friction coefficient of 0.1 (10%).

Templer	$\mathbf{v_0}$ $[m/s]$	$\mathbf{v_{r,exp}}$ $[m/s]$	$\mathbf{v_{r,sim}}$ $[m/s]$	**Error** [%]
O	348	0	50	-
	486	335	338	0.9
	624	511	514	0.6
	762	671	668	-0.4
	900	830	833	0.4
T4	506	0	80	-
	605	341	329	-3.5
	703	498	515	3.4
	802	632	653	3.3
	900	753	774	2.8
T6	562	0	151	-
	646	354	361	2.0
	731	504	502	-0.4
	815	627	628	0.2
	900	740	742	0.3
T7	529	0	160	-
	622	360	360	0
	715	515	514	-0.2
	807	643	646	0.5
	900	761	765	0.5

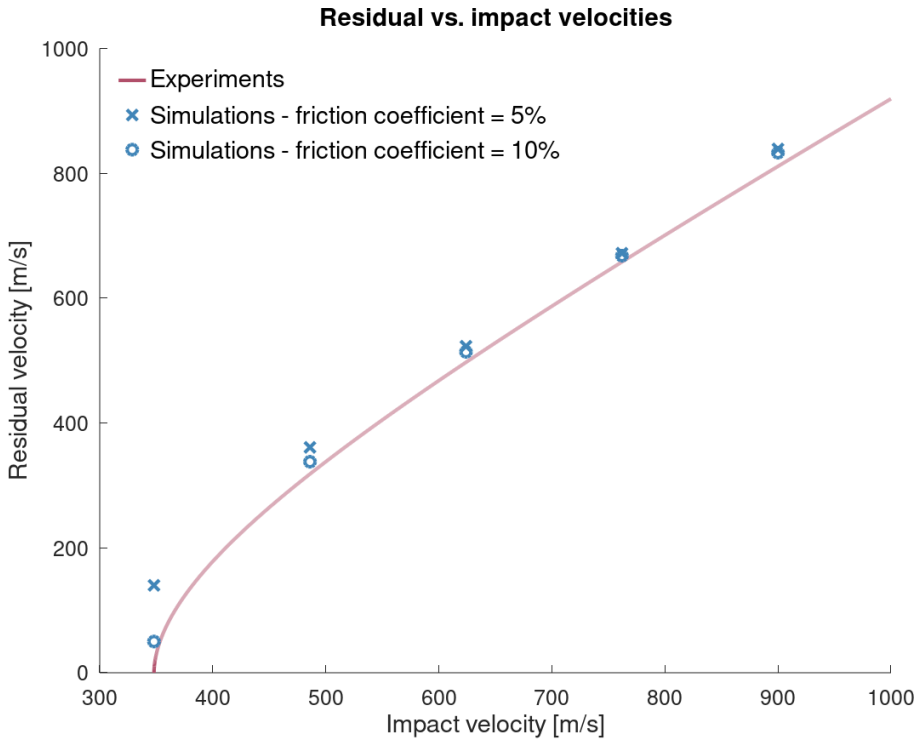

Figure 10: Residual velocities from simulations and experiments with temper O.

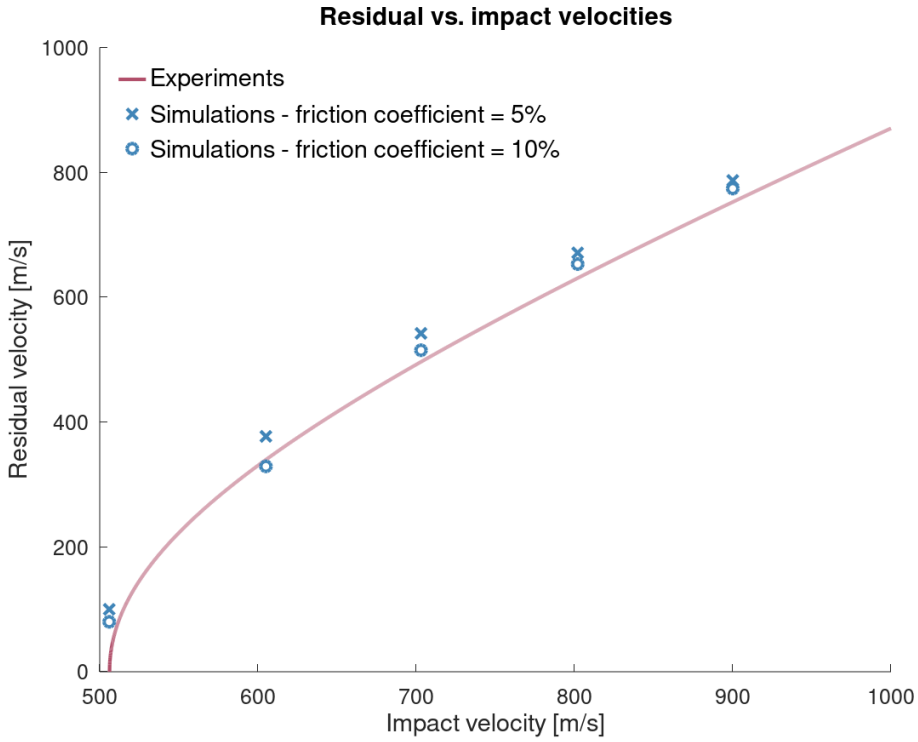

Figure 11: Residual velocities from simulations and experiments with temper T4.

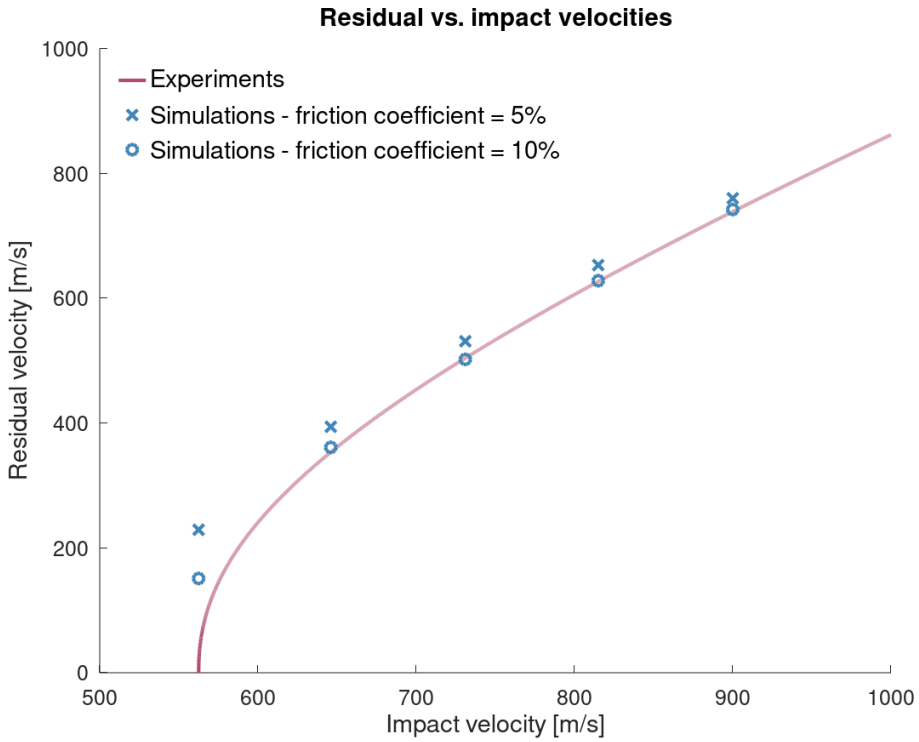

Figure 12: Residual velocities from simulations and experiments with temper T6.

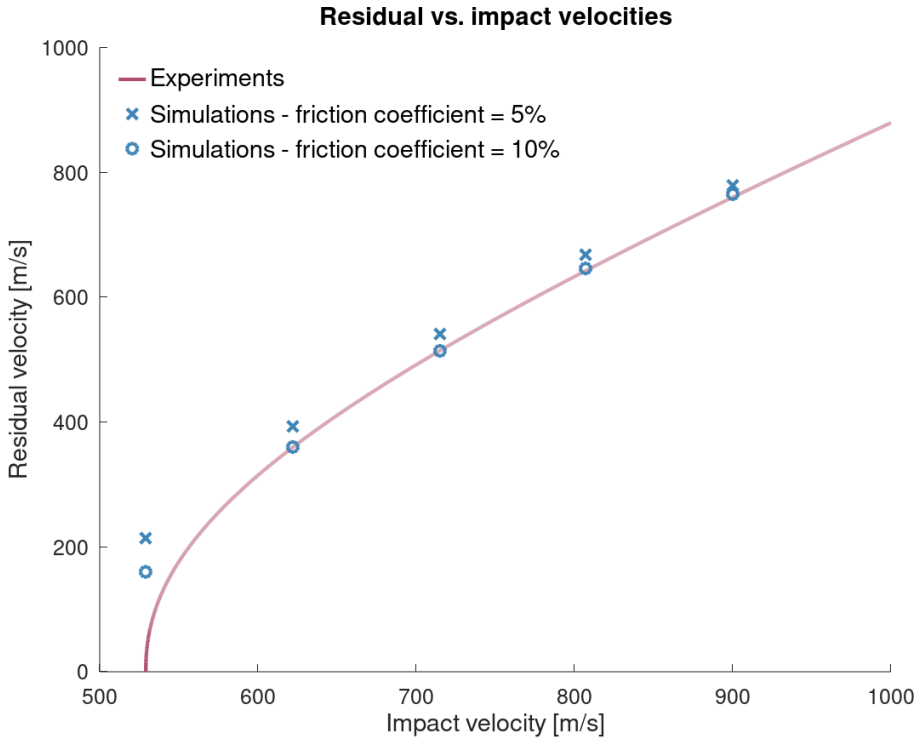

Figure 13: Residual velocities from simulations and experiments with temper T7.

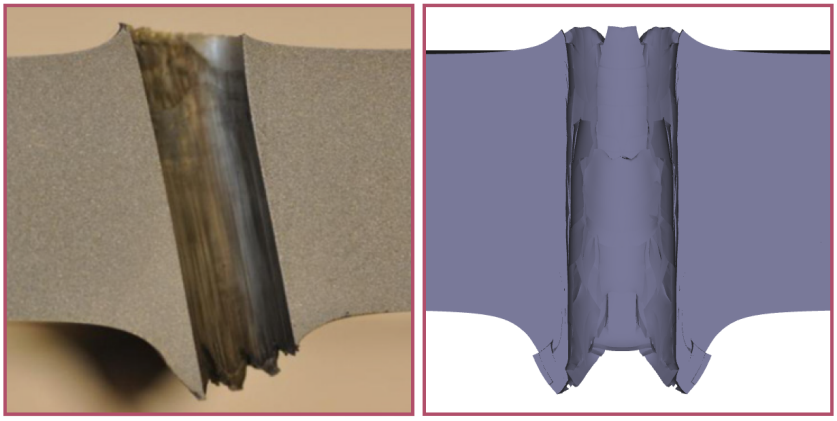

Figure 14: Temper O, impact velocity = 377 m/s.

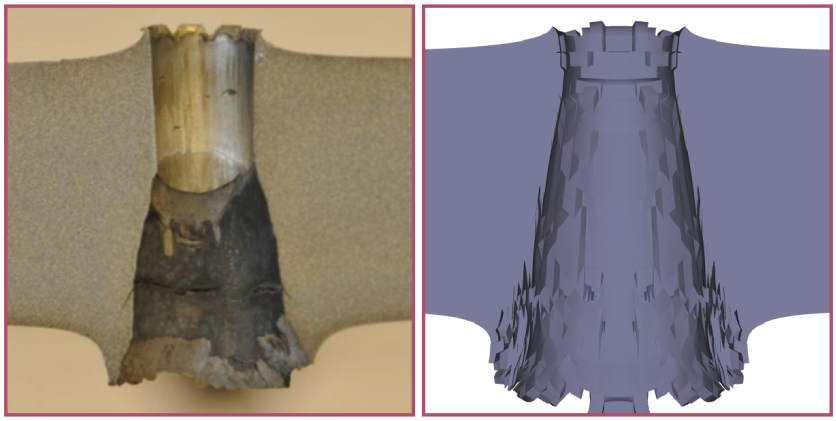

Figure 15: Temper O, impact velocity = 900 m/s.

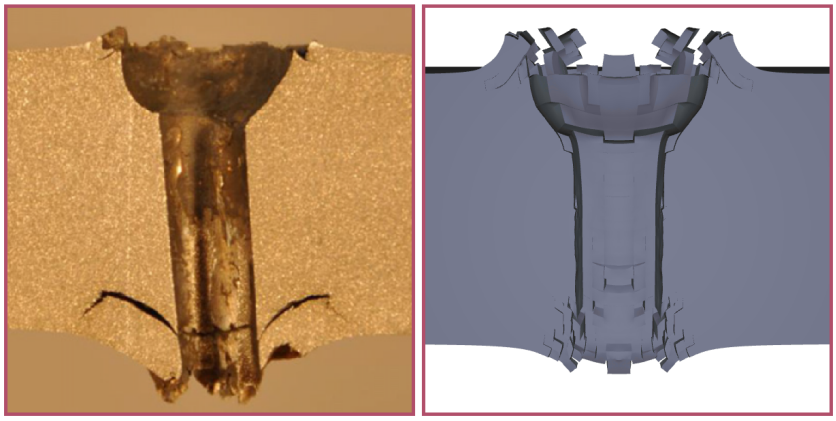

Figure 16: Temper T6, impact velocity = 589 m/s.

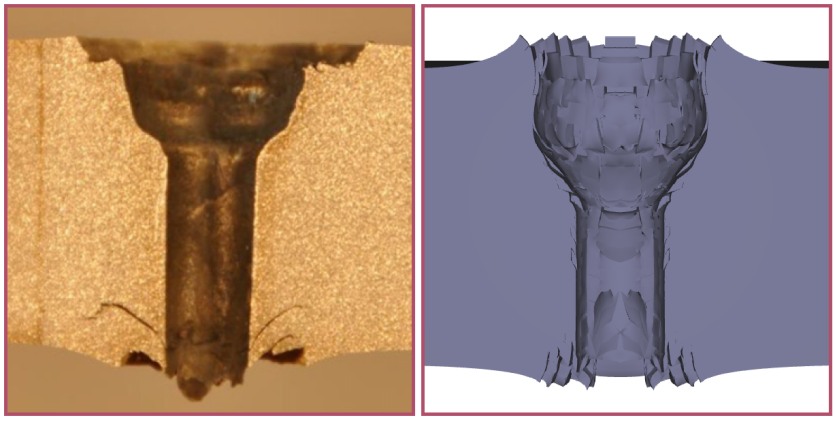

Figure 17: Temper T6, impact velocity = 662 m/s.

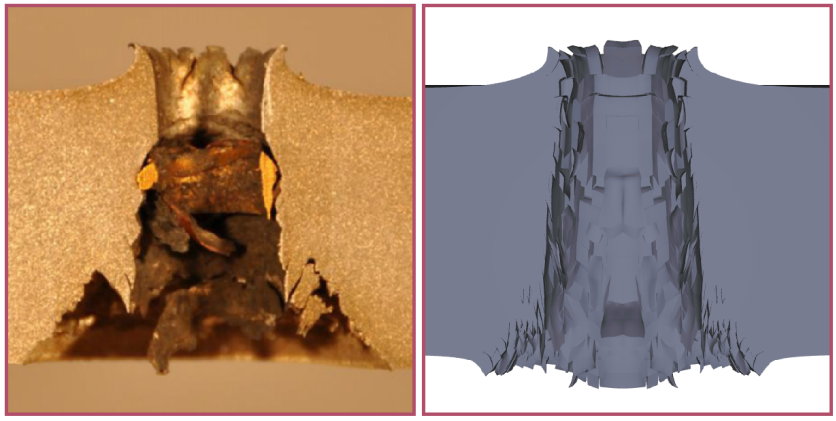

Figure 18: Temper T6, impact velocity = 903 m/s.

One simulation of each temper is subjected to version control.

References

1 - J. K. Holmen, J. Johnsen, S. Jupp, O.S. Hopperstad, T. Børvik, Effects of heat treatment on the ballistic properties of AA6070 aluminium alloy, International Journal of Impact Engineering, Volume 57, 2013, Pages 119-133.

2 - T. Børvik, S. Dey, A.H. Clausen, Perforation resistance of five different high-strength steel plates subjected to small-arms projectiles, International Journal of Impact Engineering, Volume 36, 2009, Pages 948-964.

Tests

This benchmark is associated with 4 tests.

J. P. Riegel III and D. Davison (2016)

Consistent constitutive modeling of metallic target penetration using empirical, analytical, and numerical penetration models

Ballistic tests with tungsten alloy projectiles in RHA targets are investigated experimentally by V. Hohler and A. J. Stilp (1991). Experimental results from this investigation are gathered from J. P. Riegel III and D. Davison (2016) [1].

Cylindrical projectiles with length L = 58.0 mm and a diameter D = 5.8 mm impact semi-infinite targets of RHA with impact velocities in the range of 500 - 2100 m/s. The target is modeled as a cylinder with a diameter equal to 20D and a length equal to 3L.

The targets are constructed of three layers in the numerical model. The outermost layer (0.0 - 6.35 mm) is modeled with the calibration of 12.7 mm thick material. The intermediate layer (6.35 - 19.05 mm) with the calibration of 38.1 mm thick material and the innermost layer (19.05 - 174.0 mm) with the calibration of 101.6 mm thick material. The projectile is modeled with the tungsten alloy grade Y925 with the density changed to 17 600 $kg/m3$.

Model settings:

- Cubic elements with a side-length of approximately 1.5 mm are used in the impact zone and the projectile.
- Axi-symmetry is used as displayed in Figure 19.
- The backside of the target is fixed in the direction of impact.
- A deviatoric erosion strain of 3.0 (300%) is used to maintain a reasonable time step size.
- The friction coefficient is set to 0.02 (2%).

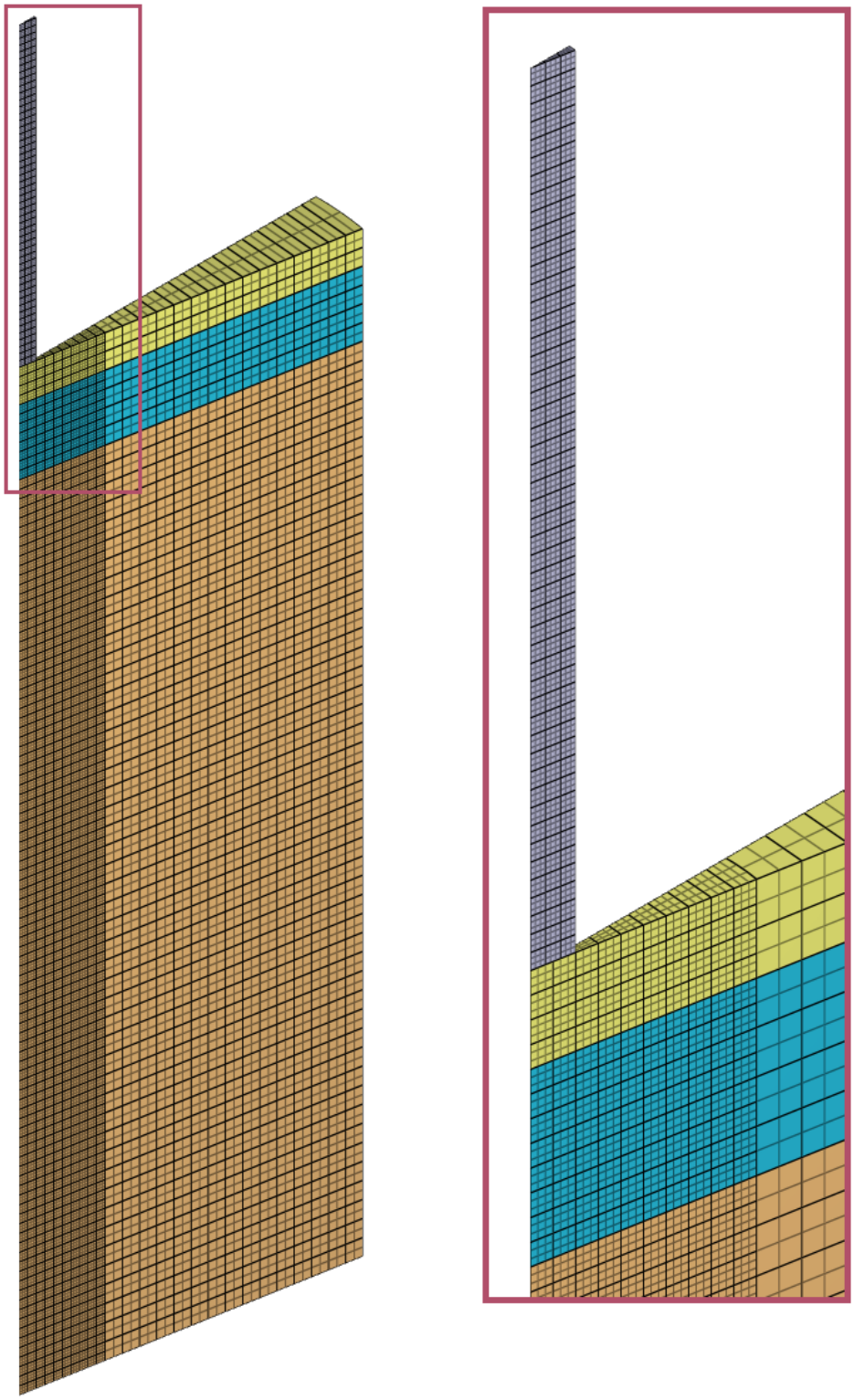

Figure 19: Axi-symmetric model of the RHA target and the tungsten alloy projectile. Different RHA calibrations are applied to different parts of the target.

Penetration depths are presented in Table 7 and Figure 20 together with data from experiments.

Table 7: Penetration depths in experiments and simulations at different impact velocities.

Impact velocity $[m/s]$	**Penetration depth - exp.** $[mm]$	**Penetration depth - sim.** $[mm]$	**Error** $[\%]$
500	2.0	2.0	0.0
1000	20.9	21.9	4.8
1500	52.3	55.4	6.0
2000	74.6	76.1	2.0

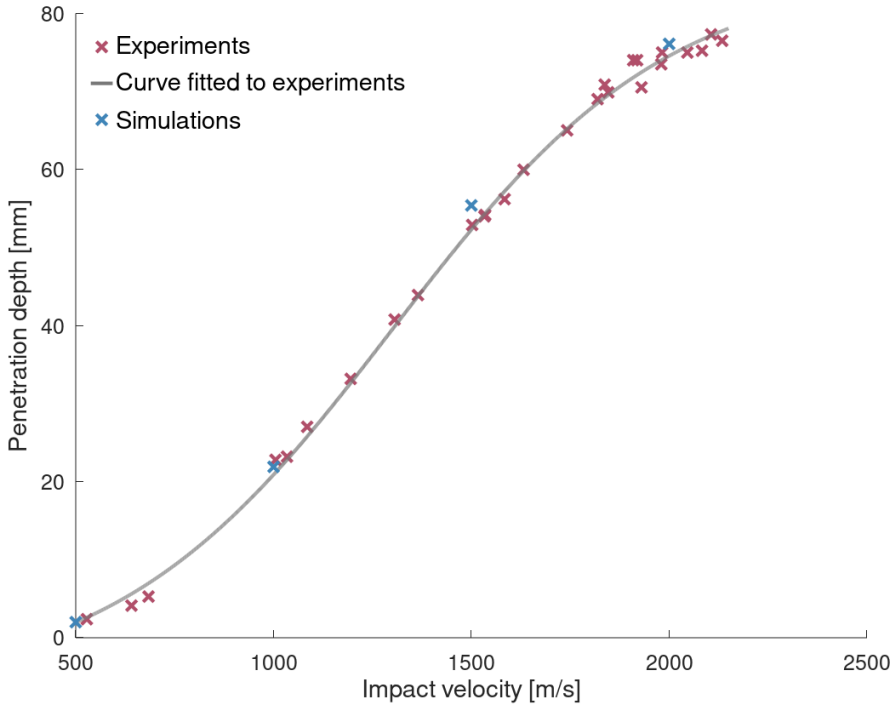

Figure 20: Penetration depths in experiments and simulations at different impact velocities.

The case with an impact velocity of 1500 m/s is subjected to version control.

References

1 - J. P. Riegel III and D. Davison, Consistent constitutive modeling of metallic target penetration using empirical, analytical, and numerical penetration models, Defence Technology 12, pages 201-213, 2016.

Tests

This benchmark is associated with 1 tests.

K. Karthikeyan et al. (2013)

The effect of shear strength on the ballistic response of laminated composite plates

Deflection profiles from experiments with Dyneema HB26 plates impacted by steel balls are presented in K. Karthikeyan et al. [1]. A numerical model of the experiments is created and deflection profiles from the simulations are compared to profiles from the experiments.

Target plate dimensions are 150 x 150 x 6 mm and the plate is clamped between two circular steel rings with an inner diameter of 100 mm, outer diameter of 150 mm and a thickness of 6.35 mm. The 8.3 g steel ball has a diameter of 12.7 mm and impacts the target plate at 250 m/s.
Model settings:

- Investigated layer thicknesses are 1 and 2 mm (cf. 0.25 mm per layer product).
- One element through the thickness of each layer.
- Steel ball is modeled as elastic with E = 210 GPa, nu = 0.3 and rho = 7740 kg/m^3
- Third order hexahedrons are used exclusively.
- Adhesive properties between layers is defined with *MERGE and *MERGE_FAILURE_COHESIVE.
- Quarter symmetry is utilized as visible in Figure 21.
- A deviatoric erosion strain of 3.0 (300%) is used.
- The friction coefficient is set to 0.025 (2.5%).

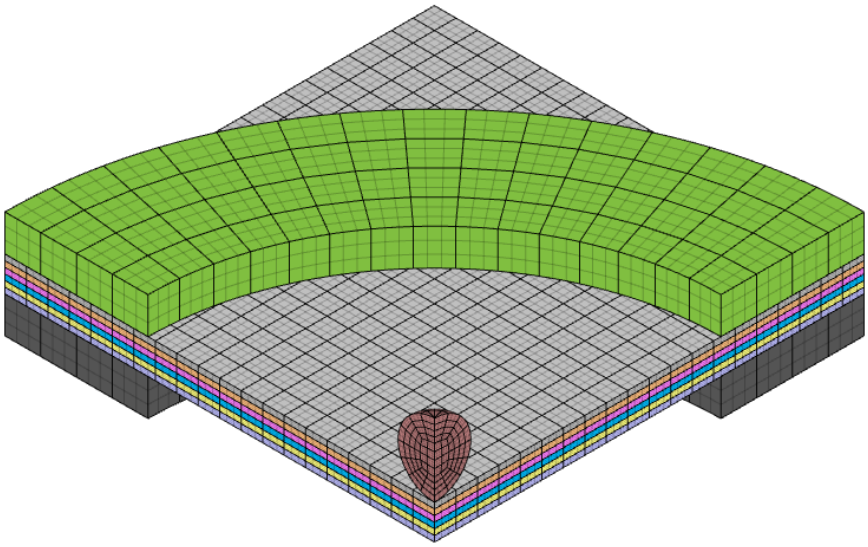

Figure 21: Quarter symmetry model of the Dyneema HB26 plate clamped between the two steel rings.

Deflection profiles at different times after impact found from the simulations are compared to profiles from the experiments in Figure 22. The profiles are registered at the following times (smallest to greatest displacements): 23, 47, 71, 95 and 142 μs.

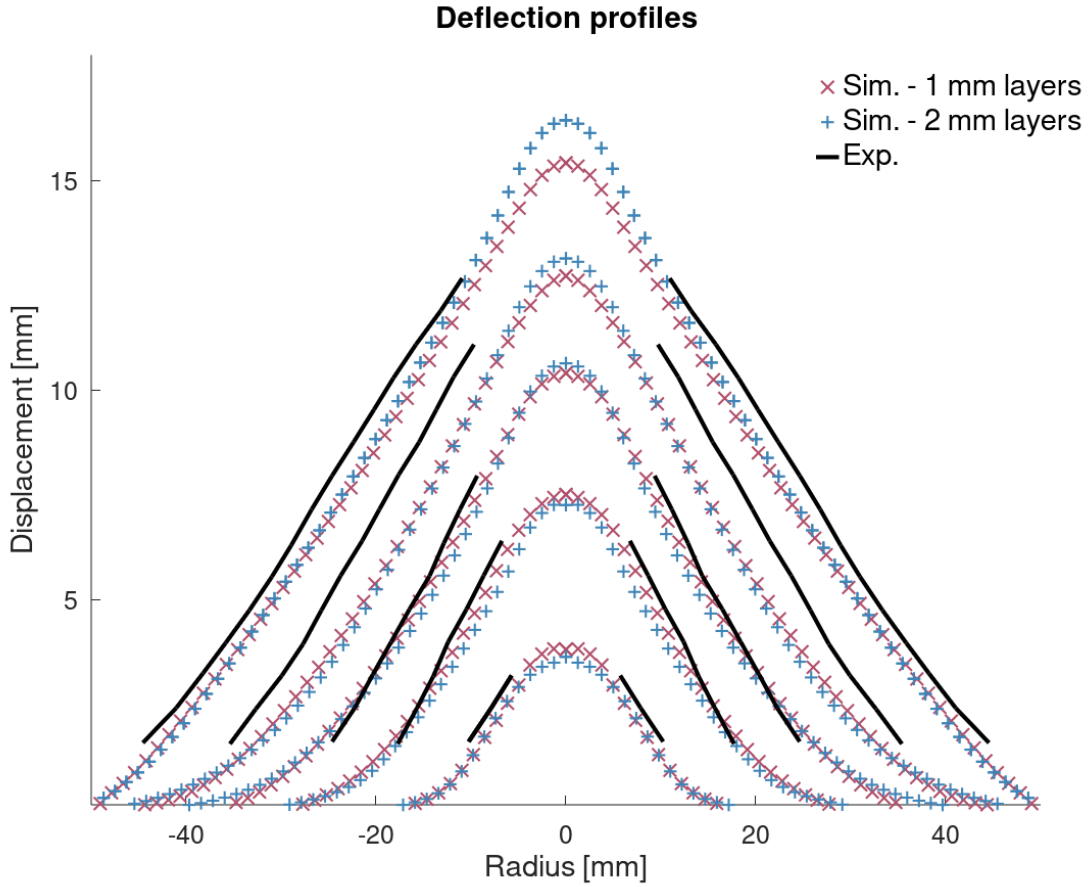

Figure 22: Deflection profiles from simulations compared to profiles from experiment.

The model with 2 mm layers is subjected to version control.

References

1 - The effect of shear strength on the ballistic response of laminated composite plates, K. Karthikeyan et al. European Journal of Mechanics A/solids, pages 35-53, 2013.

Tests

This benchmark is associated with 1 tests.

L. H. Nguyen et al. (2016)

A methodology for hydrocode analysis of ultra-high molecular weight polyethylene composite under ballistic impact

Residual vs. impact velocity and apex displacement vs. time from ballistic experiments on Dyeema HB26 are presented in L. H. Nguyen et al. (2016) [1]. Square target plates with a side length of 300 mm and a thickness of 10, 20 and 36.2 mm are impacted by a 20 mm FSP (Fragment Simulating Projectile). The material object of Dyneema HB26 is used in the numerical models and the models are evaluated against the experimental results.

Model settings:

- Investigated layer thicknesses are 1 and 2 mm for each target plate (cf. 0.25 mm per layer product).
- One element through the thickness of each layer.
- Second order hexahedrons are used exclusively.
- Surfaces with a normal in the X- or Y-direction are free in the X- and Y-direction while fixed in the Z-direction.
- Adhesive properties between layers are defined with *MERGE and *MERGE_FAILURE_COHESIVE.
- Quarter symmetry is utilized as visible in Figure 23.
- A deviatoric erosion strain of 3.0 (300%) is used.
- The friction coefficient is set to 0.025 (2.5%).

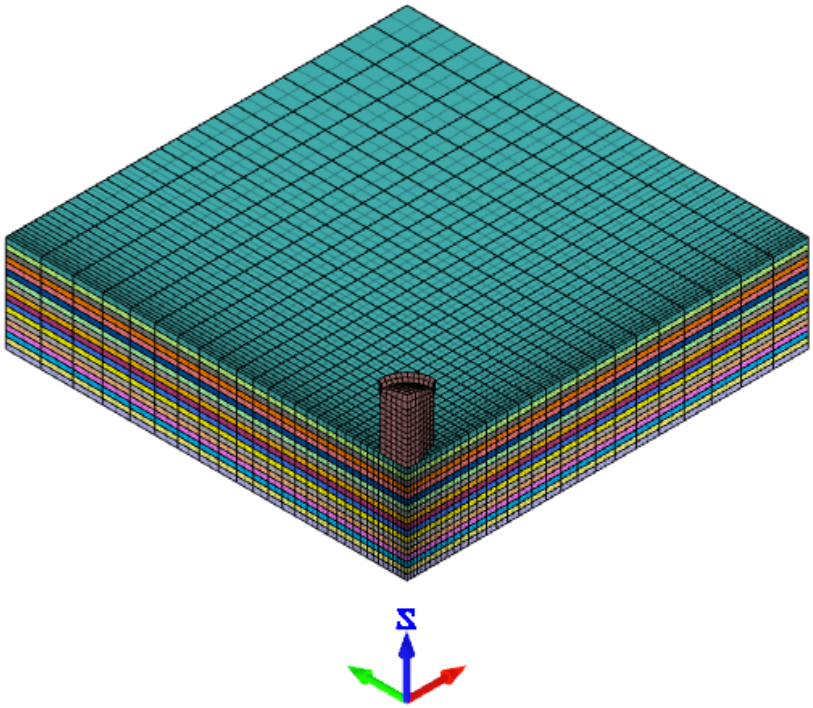

Figure 23: Quarter symmetry model of the 20 mm FSP and the 36.2 mm thick target plate.

Experimental data of the residual vs. impact velocities are available for the 10 and 20 mm target plates. Ballistic limit velocities and apex displacements are available for all plate thicknesses. Comparisons between numerical and experimental residual velocities are presented in Table 8, Table 9 and Figure 24. Ballistic limit velocity, v_{bl}, is investigated using impact velocities of $0.9 \cdot v_{bl}$ and $1.1 \cdot v_{bl}$. Results from these simulations are presented in Table 10 - 12. The comparisons of the apex displacements are presented in Figure 25 - 27.

Table 8: Residual velocities from simulations, $v_{r,sim}$, and experiments, $v_{r,exp}$, at different impact velocities, v_i, for the 10 mm target plate.

		Layer thickness = 2 mm		Layer thickness = 1 mm	
$\mathbf{v_i}$ $[m/s]$	$\mathbf{v_{r,exp}}$ $[m/s]$	$\mathbf{v_{r,sim}}$ $[m/s]$	**Error** $[\%]$	$\mathbf{v_{r,sim}}$ $[m/s]$	**Error** $[\%]$
418	102	224.3	119.9	155.0	52.0
441	263	276.6	5.2	310.8	18.2
464	352	344.4	-2.2	358.4	1.8
643	583	550.5	-5.6	573.9	-1.6
984	952	916.7	-3.7	919.0	-3.5

Table 9: Residual velocities from simulations, $v_{r,sim}$, and experiments, $v_{r,exp}$, at different impact velocities, v_i, for the 20 mm target plate.

		Layer thickness = 2 mm		Layer thickness = 1 mm	
$\mathbf{v_i}$ $[m/s]$	$\mathbf{v_{r,exp}}$ $[m/s]$	$\mathbf{v_{r,sim}}$ $[m/s]$	**Error** $[\%]$	$\mathbf{v_{r,sim}}$ $[m/s]$	**Error** $[\%]$
683	447	456.2	2.1	470.8	5.3
899	737	747.2	1.4	746.8	1.3
1058	866	916.0	5.7	920.5	6.3

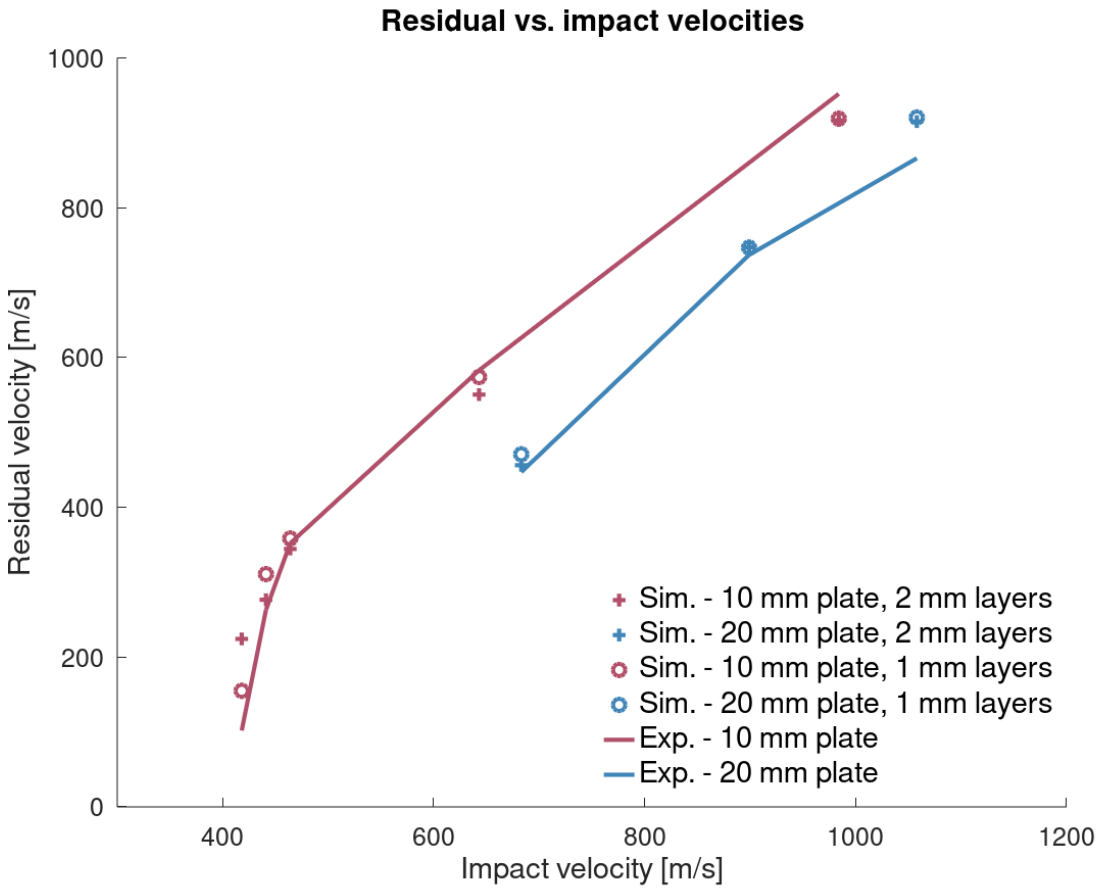

Figure 24: Residual vs. impact velocities for the 10 and 20 mm target plates. Simulations are run with both 1 and 2 mm thick layers.

Table 10: Ballistic limit velocities, v_{bl}, found from experiments together with residual velocities from simulations, $v_{r,sim}$, at impact velocities, $v_i = 0.9 \cdot v_{bl}$ and $v_i = 1.1 \cdot v_{bl}$ for the 10 mm thick plate.

		Layer thickness = 2 mm	Layer thickness = 1 mm
$\mathbf{v_{bl}}$ $[m/s]$	$\mathbf{v_i}$ $[m/s]$	$\mathbf{v_{r,sim}}$ $[m/s]$	$\mathbf{v_{r,sim}}$ $[m/s]$
394	$0.9 \cdot v_{bl}$	0.0	0.0
394	$1.1 \cdot v_{bl}$	290.8	279.2

Table 11: Ballistic limit velocities, v_{bl}, found from experiments together with residual velocities from simulations, $v_{r,sim}$, at impact velocities, $v_i = 0.9 \cdot v_{bl}$ and $v_i = 1.1 \cdot v_{bl}$ for the 20 mm thick plate.

		Layer thickness = 2 mm	Layer thickness = 1 mm
$\mathbf{v_{bl}}$ $[m/s]$	$\mathbf{v_i}$ $[m/s]$	$\mathbf{v_{r,sim}}$ $[m/s]$	$\mathbf{v_{r,sim}}$ $[m/s]$
620	$0.9 \cdot v_{bl}$	0.0	0.0
620	$1.1 \cdot v_{bl}$	452.2	468.8

Table 12: Ballistic limit velocities, v_{bl}, found from experiments together with residual velocities from simulations, $v_{r,sim}$, at impact velocities, $v_i = 0.9 \cdot v_{bl}$ and $v_i = 1.1 \cdot v_{bl}$ for the 36.2 mm thick plate.

		Layer thickness = 2 mm	Layer thickness = 1 mm
$\mathbf{v_{bl}}$ $[m/s]$	$\mathbf{v_i}$ $[m/s]$	$\mathbf{v_{r,sim}}$ $[m/s]$	$\mathbf{v_{r,sim}}$ $[m/s]$
901	$0.9 \cdot v_{bl}$	0.0	0.0
901	$0.9 \cdot v_{bl}$	624.2	636.1

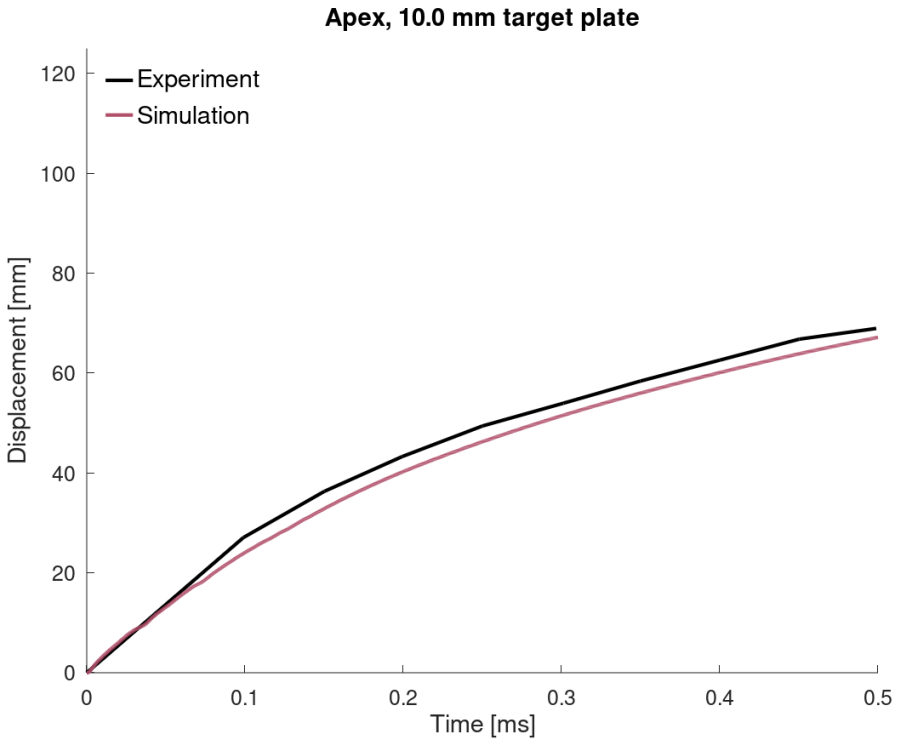

Figure 25: Apex displacement from simulation and experiment for the 10 mm target plate. The impact velocity is 394 m/s and the model is run with 1 mm layers.

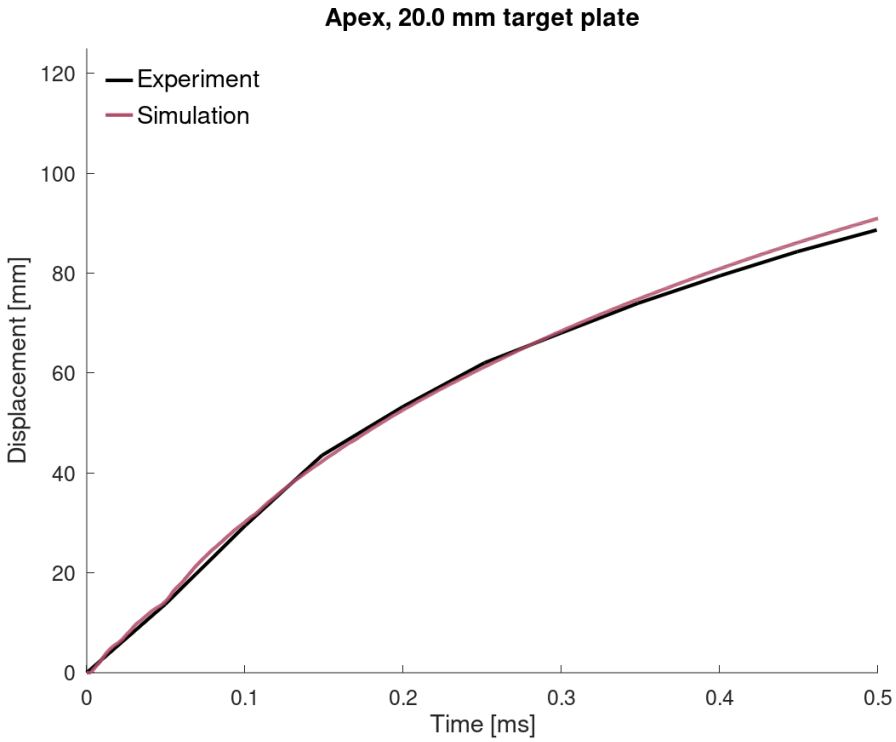

Figure 26: Apex displacement from simulation and experiment for the 20 mm target plate. The impact velocity is 615 m/s and the model is run with 1 mm layers.

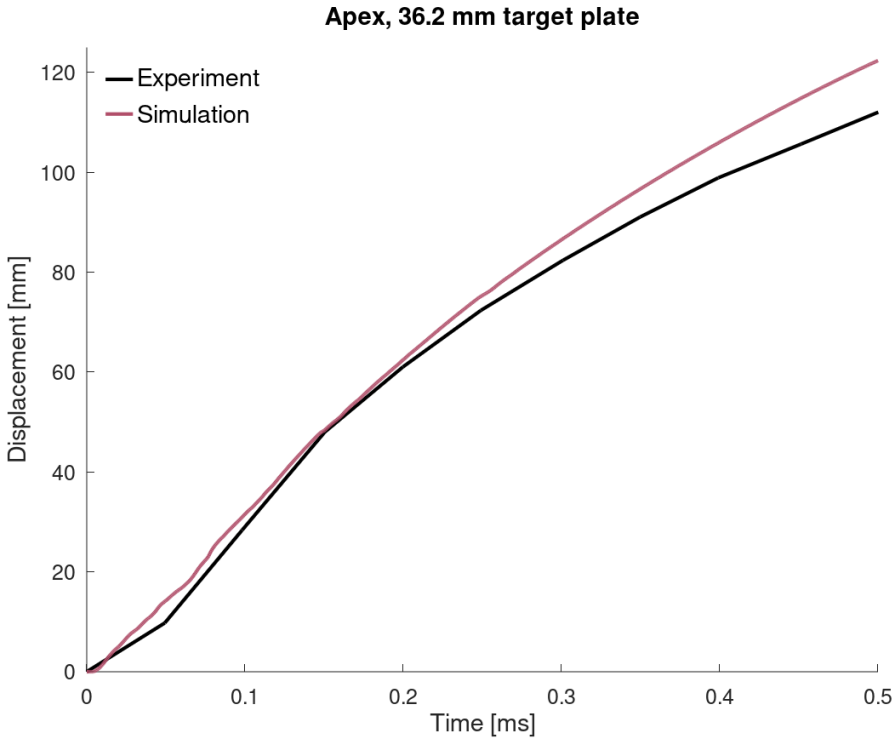

Figure 27: Apex displacement from simulation and experiment for the 36.2 mm target plate. The impact velocity is 888 m/s and the model is run with 1 mm layers.

Images from the simulation with the 20 mm thick target plate are presented in Figure 28.

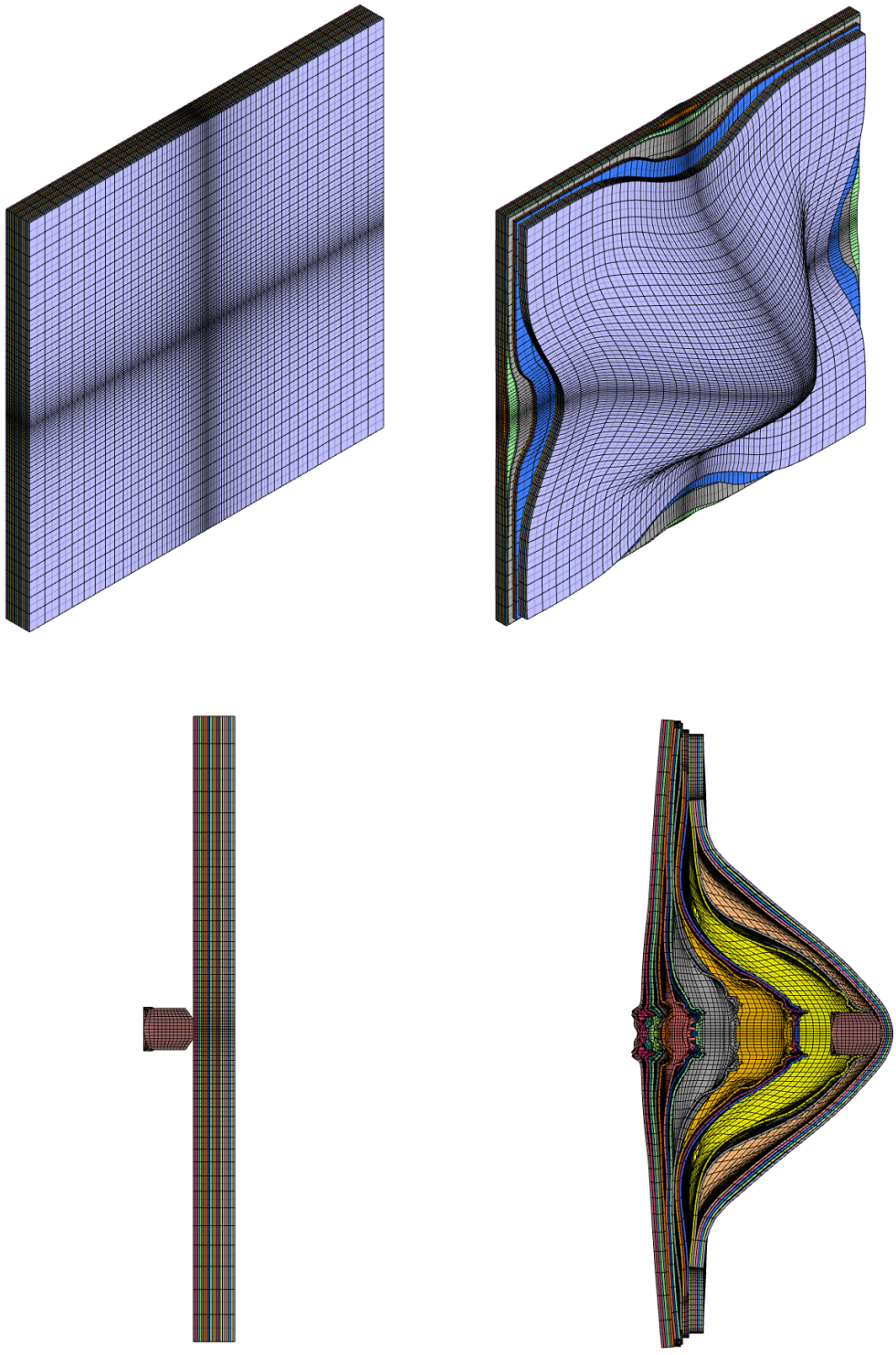

Figure 28: Isometric and side view of the 20 mm target plate modeled with 1 mm layers at initiation and termination.

Two of the simulations are subjected to version control.

References

1 - A methodology for hydrocode analysis of ultra-high molecular weight polyethylene composite under ballistic impact, L. H. Nguyen et al., Composites: Part A, pages 224-235, 2016.

Tests

This benchmark is associated with 2 tests.

P. Lundberg (2004)

Interface defeat and Penetration: Two Modes of Interaction between Metallic Projectile and Ceramic Targets

Silicon carbide (SiC-N) cylinders confined in steel (Mar 350) cups are impacted by long rod projectiles (LRP) of a wolfram heavy alloy (WHA). Experimental details and results are presented in P. Lundberg (2004) [1].

Two different types of interaction between the LRP and the SiC-target are identified:

- Interface defeat - radial flow of the LRP on the surface of the target without any significant penetration.
- Penetration - significant penetration to the target.

A transition velocity, v_{tr} = 1507 $\pm$ 5 m/s is identified in the experiments. Interface defeat is achieved for impact velocities below v_{tr} while penetration occurs for velocities higher than v_{tr}.

The diameter and height of the SiC-N cylinders is 20.0 mm. The LRP length is 80.0 mm and the diameter is 2.0 mm. Geometries of the steel cup and copper lid can be found in the referenced literature. A model of WHA grade Y925, which is the grade used in the experiments, is included from the object store together with a model of copper. The steel is modeled in accordance to [3] and the SiC-N model calibrated so far is used. Basic mechanical properties for the WHA, copper and steel is presented in Table 13.

Table 13: Material properties for the wolfram heavy alloy, copper and steel.

Material	**Density** $[kg/m^3]$	**Young's modulus** $[GPa]$	**Static yield strength** $[MPa]$
WHA	17700	340	1300
Copper	8520	115	102
Steel	8100	194	2600

Full models (w/o symmetry) with QHEX elements were used in the simulations and the simulations are done in two steps. An image of the model is presented in Figure 29

In the first step, the steel cup with initial temperature T0 is cooled to the ambient temperature (assumed to 293 K) around the SiC-N cylinder, causing a confinement pressure in the SiC-N. Details regarding the shrink-fitting process is not presented in the refererenced literature so two different T0 are investigated: 793 K and 543 K.

In the second step, the LRP is included with an initial velocity v0. Two initial velocities are investigated: 1300 and 1700 m/s.

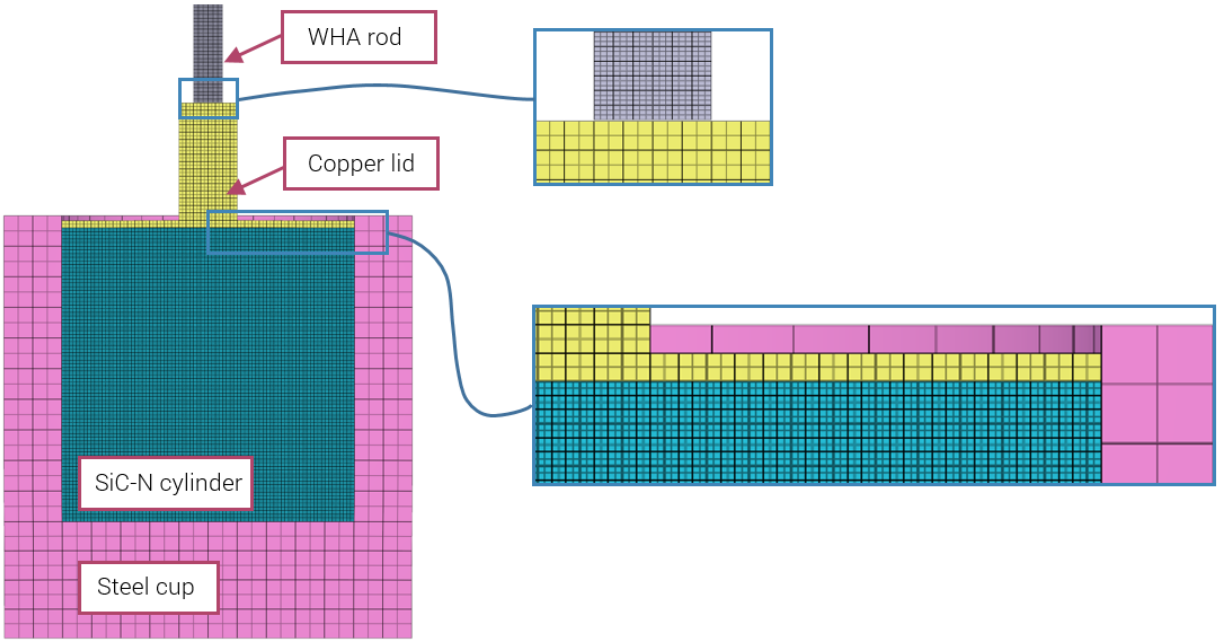

Figure 29: Cross-sectional side view of the model. Note that only a part of the projectiles entire length is displayed.

The final state of the simulations are presented in Figure 30 - 33.

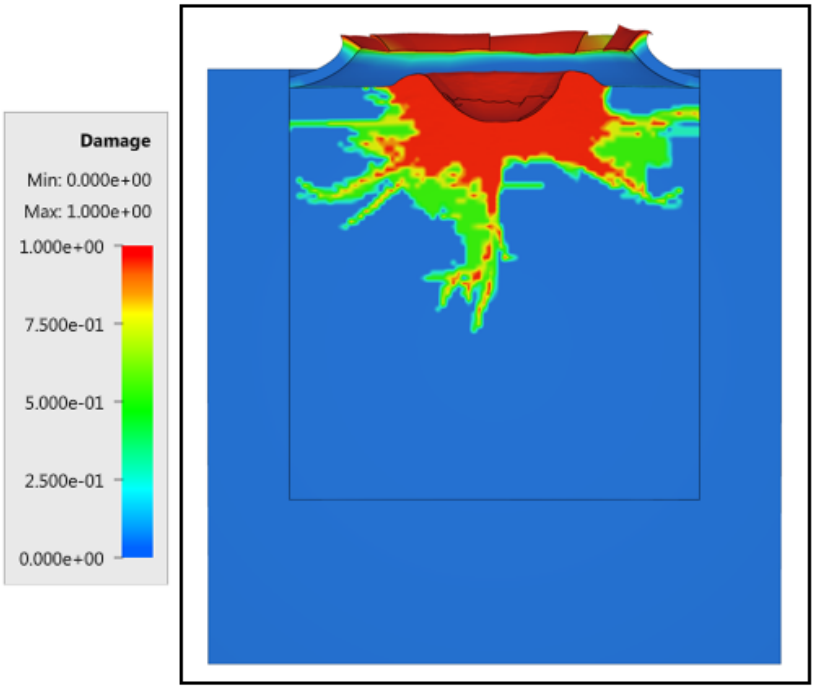

Figure 30: T_0 = 543 K, v_0= 1300 m/s

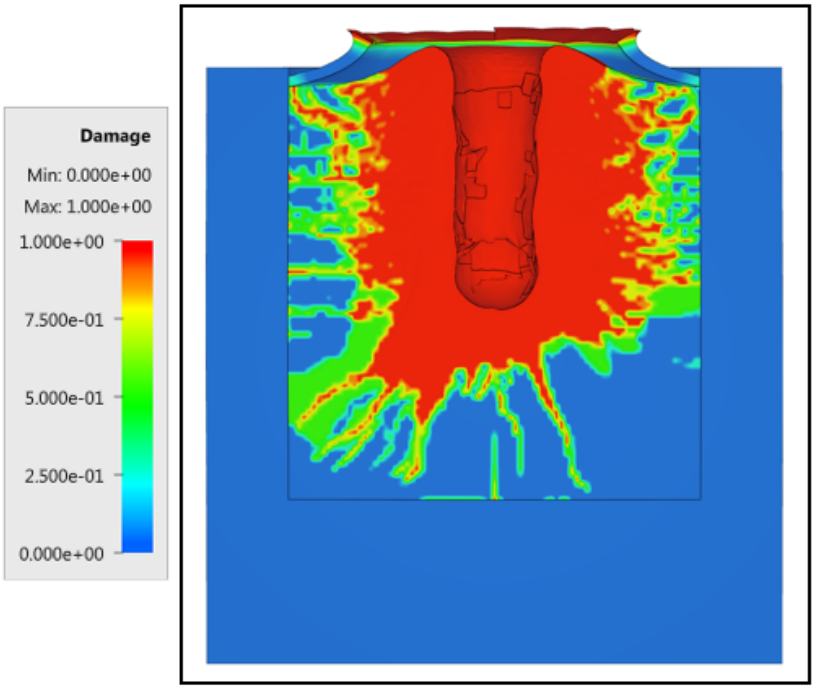

Figure 31: T_0 = 543 K, v_0= 1700 m/s

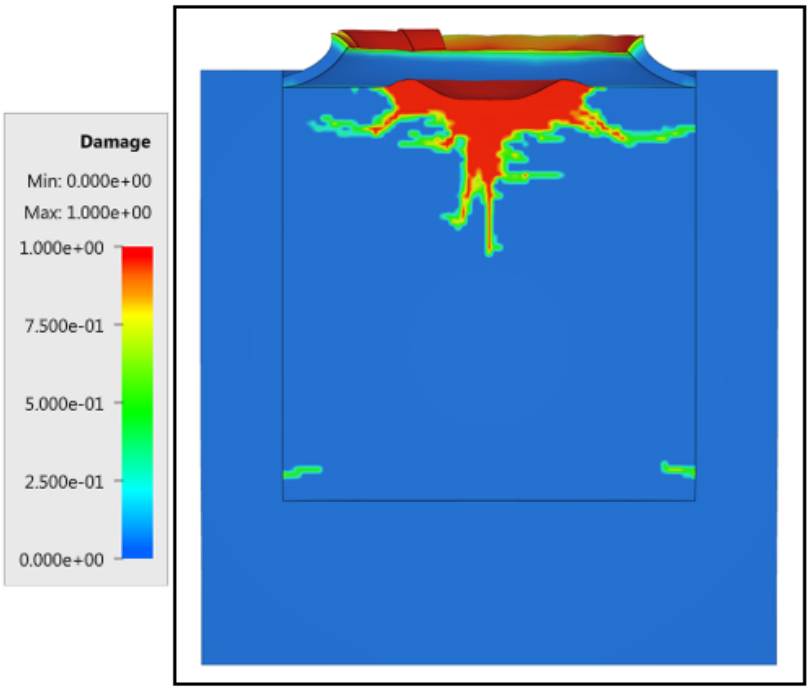

Figure 32: T_0 = 793 K, v_0= 1300 m/s

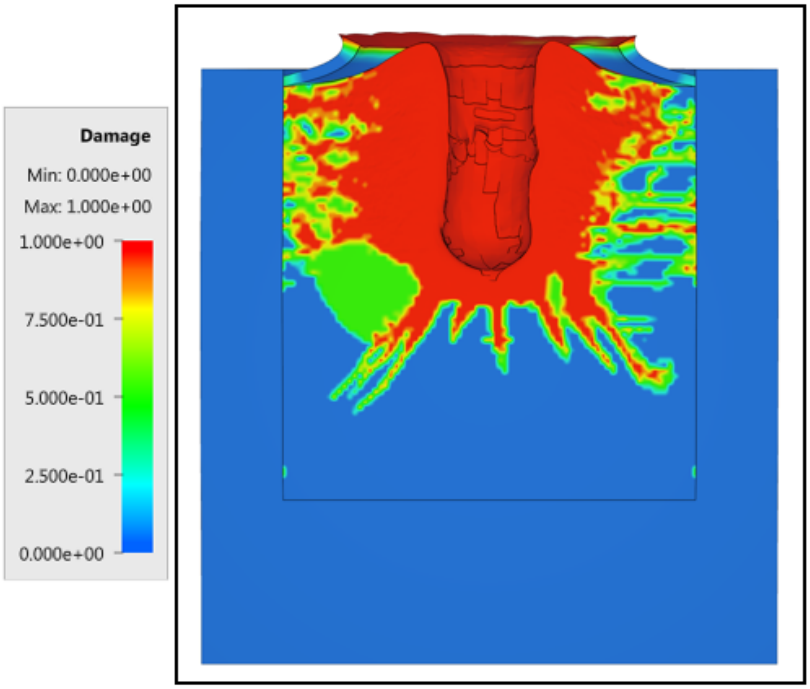

Figure 33: T_0 = 793 K, v_0= 1700 m/s

References

1 - P. Lundberg - Interface defeat and Penetration: Two Modes of Interaction between Metallic Projectile and Ceramic Targets, Dissertation from Uppsala university, 2004.

P. Weidemaier et al. (2004)

Experimental and Numerical Simulation Analysis of the Impact Process of Structured KE Penetrators onto Semi-infinite and Oblique Plate Targets

KE projectiles of WHA grade Y925 impacting semi-infinite targets of RHA (Rolled Homogeneous Armor) are experimentally investigated in P. Weidemaier et al. (2004) [1]. Projectiles with three different shapes are investigated: cylindrical, tapered conical and broadened conical. Length-to-diameter ratio equals 20 for the cylindrical projectile. The minimum diameter of the tapered and broadened projectiles is 5 mm while the maximum diameter is 8 mm. Illustrations of the different projectiles are presented in Figure 34. The mass of each projectile is 75 g and the impact velocity is 1600 m/s.

Model settings:

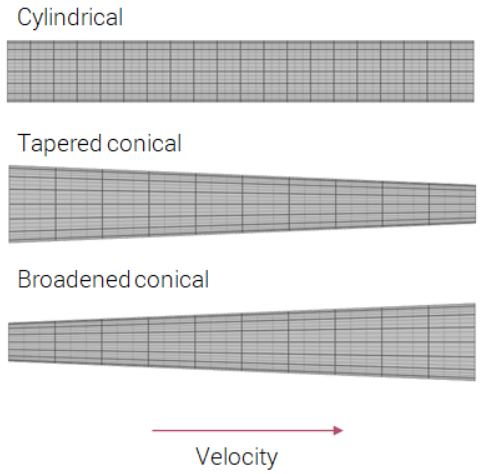

Figure 34: Illustration of the different projectile shapes.

- Third order elements are used exclusively.
- Axisymmetry is utilized and only 10° slice is modeled, as seen in Figure 35.
- Projectile modeled with 160 elements and target with 1320 elements.
- A deviatoric erosion strain of 3.0 (300%) is used to maintain a reasonable time step size.
- A friction coefficient of 0.025 (2.5%) is assumed.

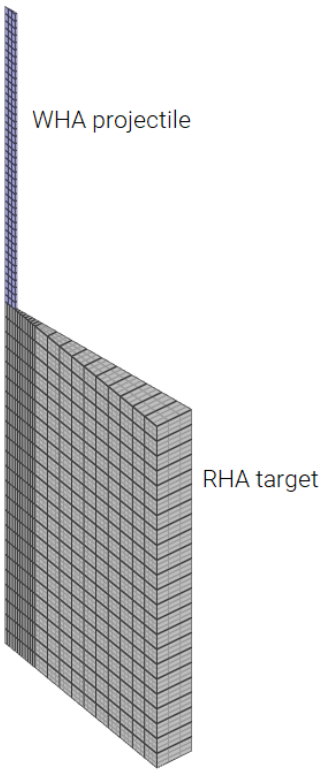

Figure 35: Axisymmetric model of WHA projectile impacting RHA target.

Penetration depths from simulations are compared to experimental values in Table 14.

Table 14: Comparison of penetration depths between simulations and experiments.

Projectile	**Penetration depth - exp.** $[mm]$	**Penetration depth - sim.** $[mm]$	**Error** $[\%]$
Cylindrical	117.2	110.8	5.8
Tapered	122.1	115.9	5.3
Broadened	109.6	103.2	6.2

The model with the cylindrical projectile is subjected to version control.

References

1 - P. Weidemaier, K. Weber, N. Heider, Experimental and Numerical Simulation Analysis of the Impact Process of Structured KE Penetrators onto Semi-infinite and Oblique Plate Targets, Ernst-Mach Institute, 2004.

Tests

This benchmark is associated with 1 tests.

S. J. Schraml (2012)

Constitutive model parameter study for armor steel and tungsten alloys

Penetration depths in blocks of RHA impacted by tungsten projectiles are investigated experimentally in S. J. Schraml (2012) [1]. A numerical model of the experiments is created to evaluate the three calibrations of RHA available in this object.

Investigated projectile length-to-diameter ratio in the experiments are 5, 10, 15 and 30. The validation work is limited to a length-to-diameter of 10. Investigated impact velocities for this setup is in the range of 1050-1750 m/s. The approximately 80 mm long projectiles with a hemispherical nose impacts RHA cubes with a side-length of 152.0 mm.

The RHA blocks are constructed of three layers in the numerical model. The outermost layer (0.0 - 6.35 mm) is modeled with the calibration of 12.7 mm thick material. The intermediate layer (6.35 - 19.05 mm) is modeled with the calibration of 38.1 mm thick material and the innermost layer (19.05 - 152.4 mm) with the calibration of 101.6 mm thick material. The projectile is modeled with the tungsten alloy grade Y925 which has a density of 17 700 kg/m^3 and is available as a material object.

Model settings:

- Hexahedron elements are used exclusively.
- Cubic elements with a side-length of 1.0 mm are used in the impact zone and the projectile.
- The depth of the mesh refinement in the target plate is set to 125% the penetration depth found from the experiments.
- Quarter symmetry is utilized as visible in Figure 36.
- The backside of the target is fixed in the direction of impact.
- A deviatoric erosion strain of 3.0 (300%) is used to maintain a reasonable time step size.
- The friction coefficient is set to 0.02 (2%).

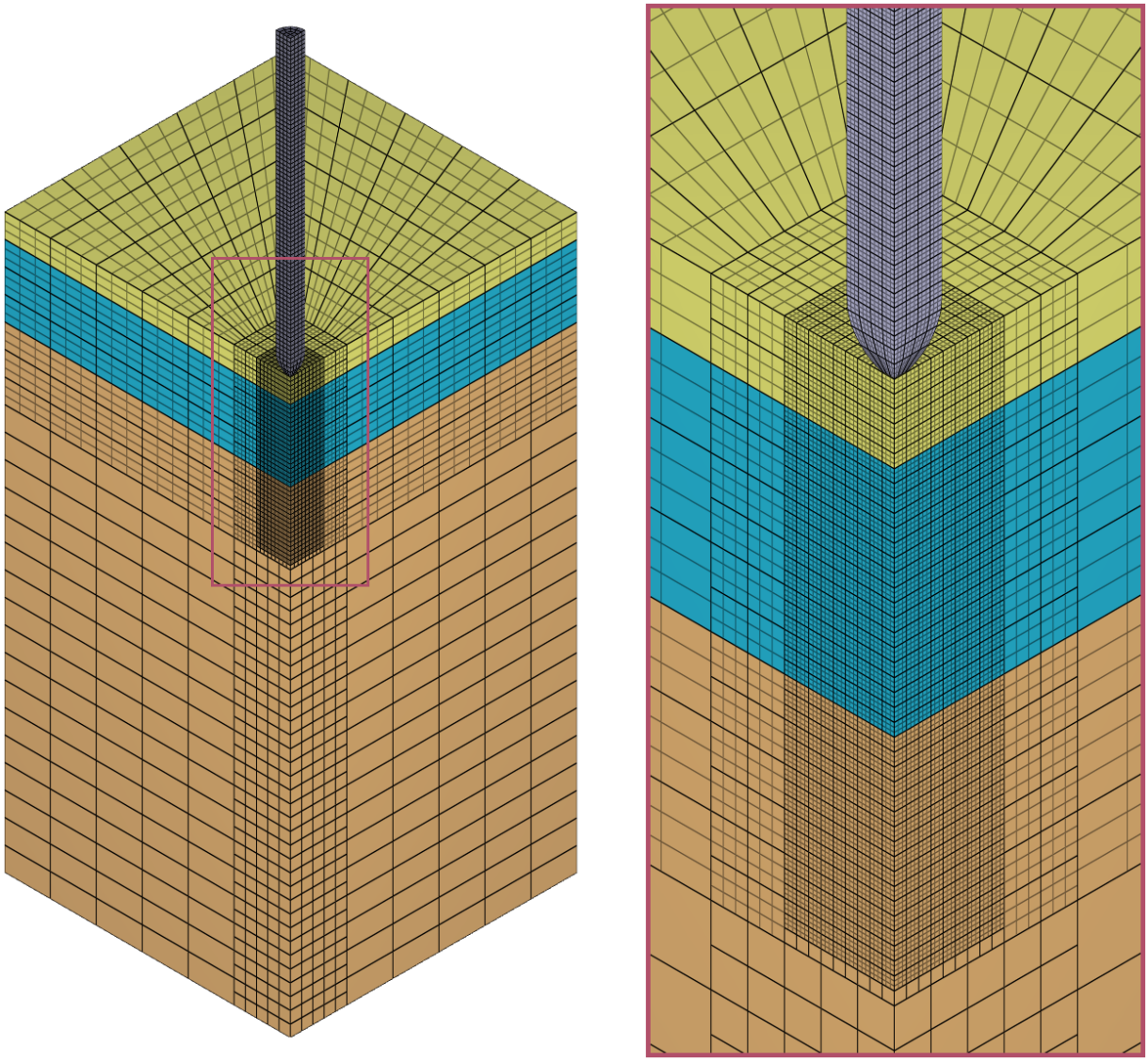

Figure 36: Quarter symmetry model of the RHA target and the tungsten alloy projectile. Different RHA calibrations are applied to different parts of the target.

Penetration depths are presented in Table 15 and Figure 37 together with data from experiments.

Table 15: Penetration depths in experiments and simulations at different impact velocities.

Impact velocity $[m/s]$	**Penetration depth - exp.** $[mm]$	**Penetration depth - sim.** $[mm]$	**Error** $[\%]$
1078	35.1	38.2	8.8
1102	37.5	40.4	7.7
1286	55.5	58.3	5.0
1298	54.9	59.0	7.5
1499	73.4	78.3	6.7
1528	75.8	81.2	7.1
1697	87.5	94.2	7.7
1718	88.3	95.4	8.0

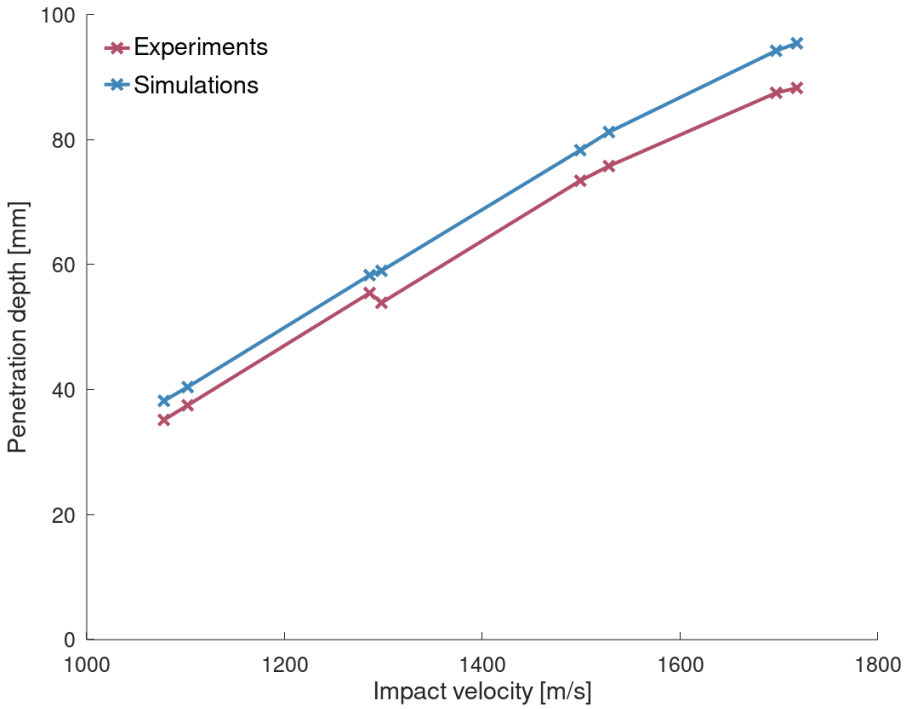

Figure 37: Penetration depths in experiments and simulations at different impact velocities.

The case with an impact velocity of 1499 m/s is subjected to version control.

References

1 - S. J. Schraml, Constitutive model parameter study for armor steel and tungsten alloys, Army research laboratory, 2012.

Tests

This benchmark is associated with 1 tests.

T. Børvik et al. (2009) (1)

Perforation of AA5083-H116 aluminium plates with conical-nose steel projectiles

Perforation experiments with conical-nose steel projectiles on plates of AA5083-H116 are presented in T. Børvik et al. (2009) [1]. A numerical model of the experiments is created to assess the calibrations of AA5083-H116 available as Material objects.

AA5083-H116 plates of different thickness are clamped in a circular frame with an inner diameter of 500 mm. A conical-nose steel projectile with length 98 mm and diameter 20 mm impacts the target plates at different velocities and the residual velocity in the case of perforation is registered. All calibrations/thicknesses are investigated numerically and compared to experimental results. The material in the projectile is modeled in accordance to the referenced literature.

Model settings:

- Third order elements in target plate and second order elements in projectile since small deformations are expected in the projectile.
- Side length of elements in the impact zone is 2.0 mm.
- Axisymmetry is utilized. A 10% slice is modeled as visible in Figure 38.
- A deviatoric erosion strain of 3.0 (300%) is used.
- A friction coefficient of 0.01 (1%) is assumed.
- No failure criterion is used.

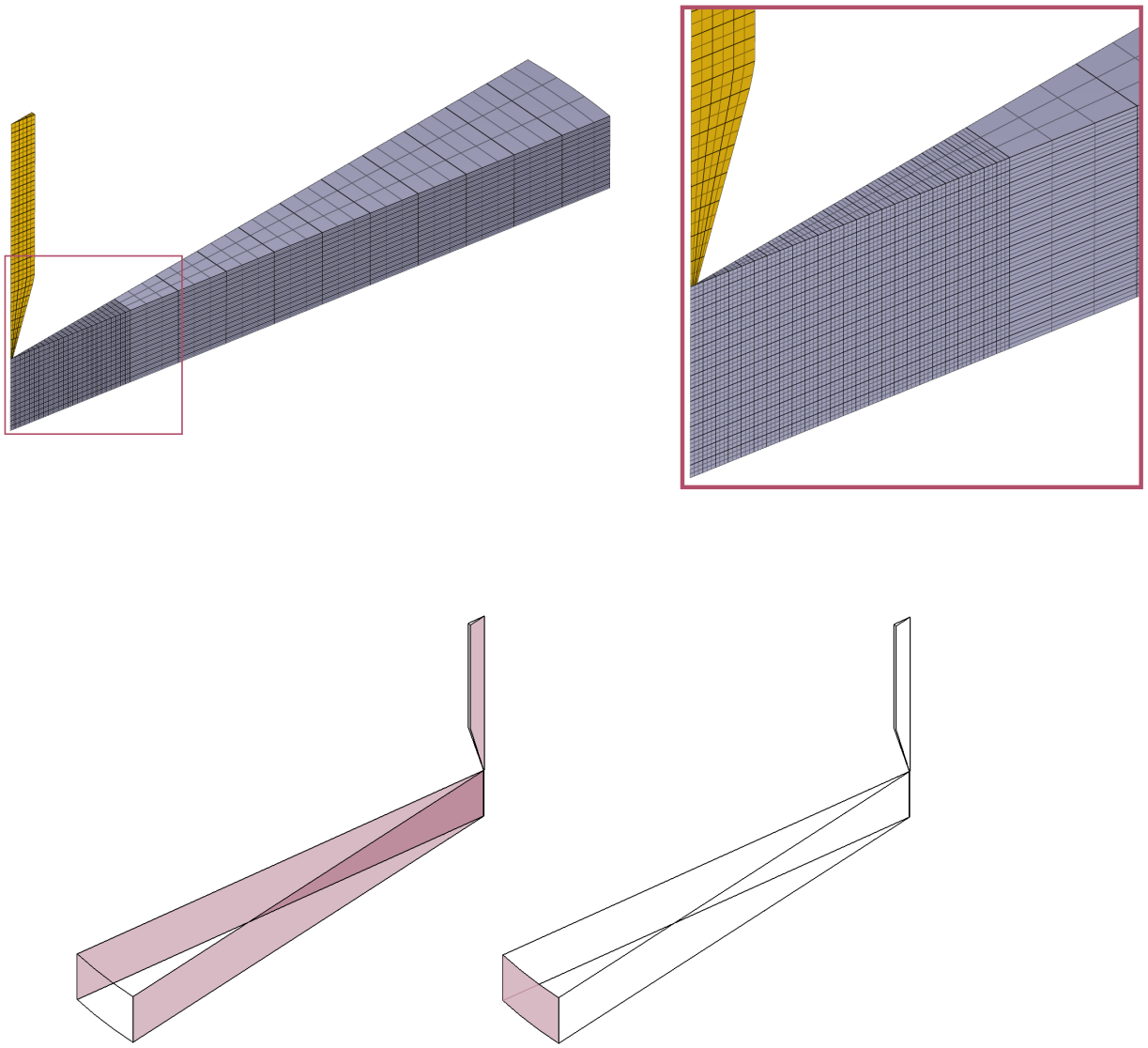

Figure 38: Axisymmetry is utilized. A finer mesh is used in the impact zone. Symmetry conditions are applied to surfaces with a normal in the tangential direction. The surface with normal in the radial direction is fixed in XYZ.

The failure mechanism seen in the experiments is ductile hole growth, which is also the case in the simulations due to the absence of failure criterion. Greatly distorted elements with significantly reduced shear resistance are however eroded.

Residual velocities from the models are compared to Recht-Ipson curves based on residual velocities found from the experiments. The results are presented in Table 16 and Figure 39.

Table 16: Residual velocities from experiment, $v_{r,exp}$, and simulations, $v_{r,sim}$, at different impact velocities, v_0.

Thickness $[mm]$	$\mathbf{v_0}$ $[m/s]$	$\mathbf{v_{r,exp}}$ $[m/s]$	$\mathbf{v_{r,sim}}$ $[m/s]$	**Error** $[\%]$
15	210	0	0	0
15	220	40	0	-
15	260	144	138	-4.2
15	305	215	213	-0.9
15	350	275	275	0
20	245	0	0	0
20	255	66	58	3.6
20	283	140	142	5.2
20	317	201	201	2.0
20	350	251	251	1.6
25	250	0	0	0
25	260	42	0	-
25	287	129	110	-14.7
25	319	190	179	-5.7
25	350	239	230	-3.8
30	305	0	0	0
30	315	59	55	-6.8
30	323	93	94	1.1
30	337	133	135	1.5
30	350	164	166	1.2

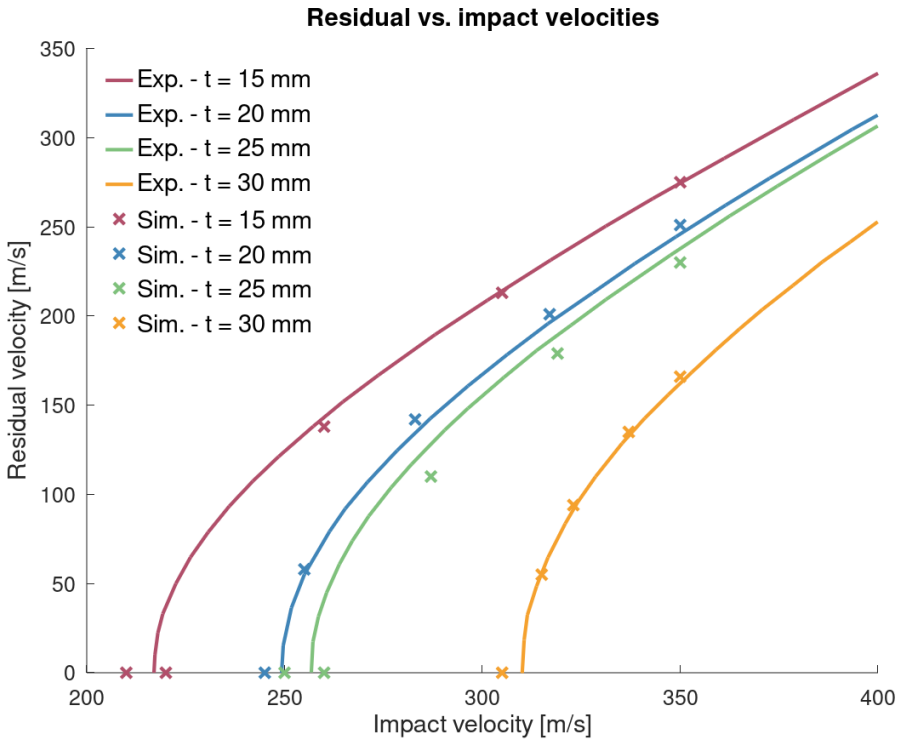

Figure 39: Residual velocities from the simulations are compared to a Recht-Ipson curve based on residual velocities from the experiments.

One simulation of each thickness/calibration is subjected to version control.

References

1 - T. Børvik, M. J. Forrestal, O. S. Hopperstad, T. L. Warren, M. Langseth, Perforation of AA5083-H116 aluminium plates with conical-nose steel projectiles - Calculations, International Journal of Impact Engineering, Volume 36, 2009, Pages 426-437.

Tests

This benchmark is associated with 4 tests.

T. Børvik et al. (2009) (2)

Perforation resistance of five different high-strength steel plates subjected to small-arms projectiles

The perforation resistance of five different high-strength steel plates against 7.62 mm APM2 projectiles is investigated in T. Børvik et al. (2009) [1]. The calibrations of Domex Protect 500, Hardox 400, Weldox 500E and Weldox 700E are added as material objects while the calibration of Armox 560T is omitted.

The target consists of two plates of the same steel with dimensions 300 x 300 x 6 mm, yielding a target thickness of 12 mm. Two opposite sides of the target are clamped while the other two sides are unconstrained. The calibrations of Domex Protect 500, Hardox 400, Weldox 500E and Weldox 700E are used in the target plate. The 7.62 mm APM2 projectile core is modeled as rigid, while models of brass and lead, which are used in the jacket and tip, are modeled in accordance to the referenced literature.

Model settings:

- Third order hexahedrons are used exclusively.
- Cubic elements with a side length of 1.0 mm are used in the impact zone.
- Quarter symmetry is utilized as visible in Figure 40.
- A deviatoric erosion strain of 3.0 (300%) is used to maintain a reasonable time step size.

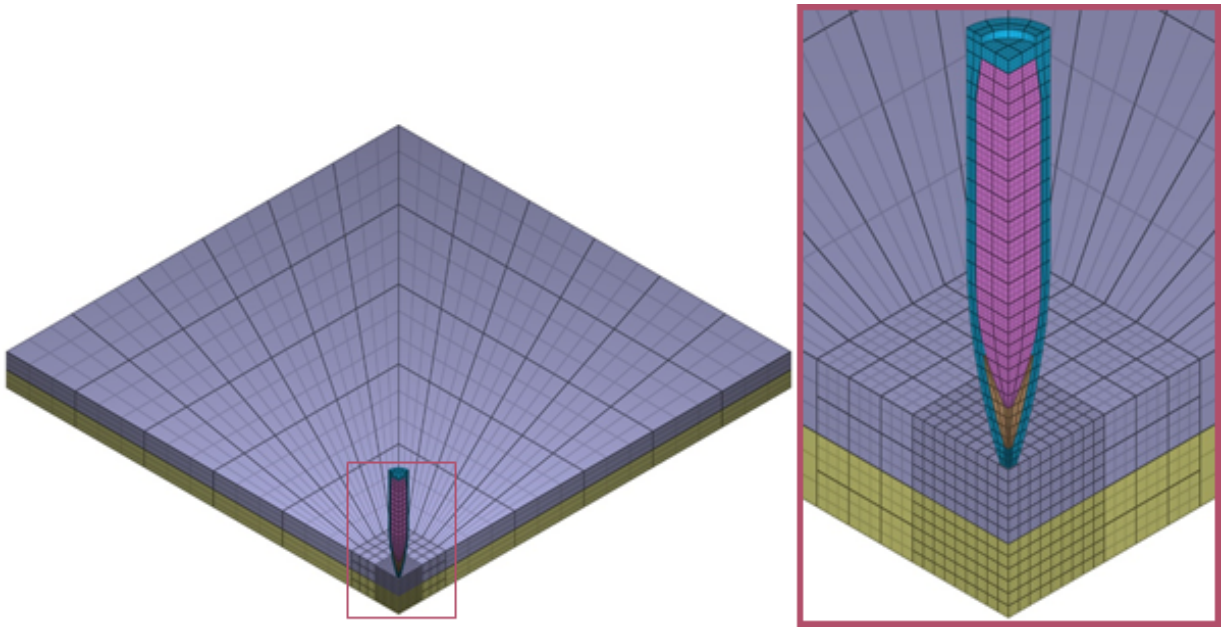

Figure 40: Quarter symmetry model of target plate and the 7.62 mm APM2 projectile. The target plate mesh is refined in the impact zone.

Five different impact velocities in the range of 600 - 1200 m/s are investigated numerically. Residual velocities from the model are compared to a Recht-Ipson curve based on residual velocities found in the experiments. Results are presented in Table 17 and Figure 41 - 44.

Table 17: Residual velocities from experiment, $v_{r,exp}$, and simulations, $v_{r,sim}$, at different impact velocities, v_0.

Material in target plate	$\mathbf{v_0}$ $[m/s]$	$\mathbf{v_{r,exp}}$ $[m/s]$	$\mathbf{v_{r,sim}}$ $[m/s]$	**Error** $[\%]$
Domex Protect 500	837	0	167	-
	897	353	350	-0.8
	957	499	473	-5.2
	1080	719	694	-3.5
	1200	894	862	-3.6
Hardox 400	742	0	0	0
	818	339	330	-2.7
	893	491	491	0.0
	1049	734	731	-0.4
	1200	936	936	0.0
Weldox 500E	623	0	152	-
	718	390	407	4.4
	813	559	551	-1.4
	1010	830	812	-2.2
	1200	1057	1038	-1.8
Weldox 700E	675	0	210	-
	762	422	443	5.0
	848	585	577	-1.4
	1027	843	815	-3.3
	1200	1058	1019	-3.7

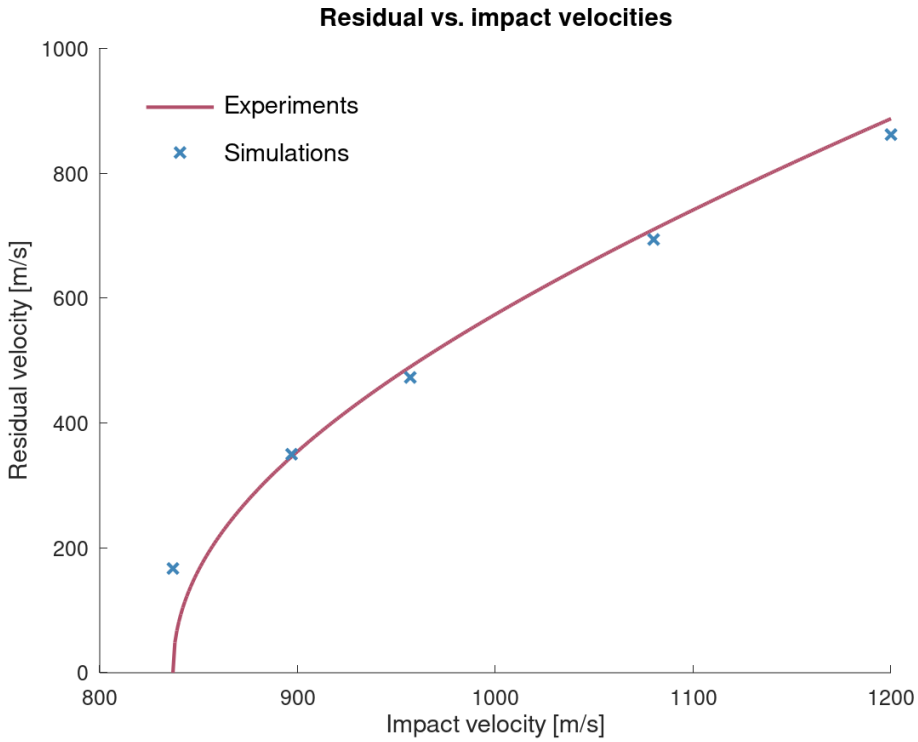

Figure 41: Residual velocities from the simulations and experiments with Domex Protect 500.

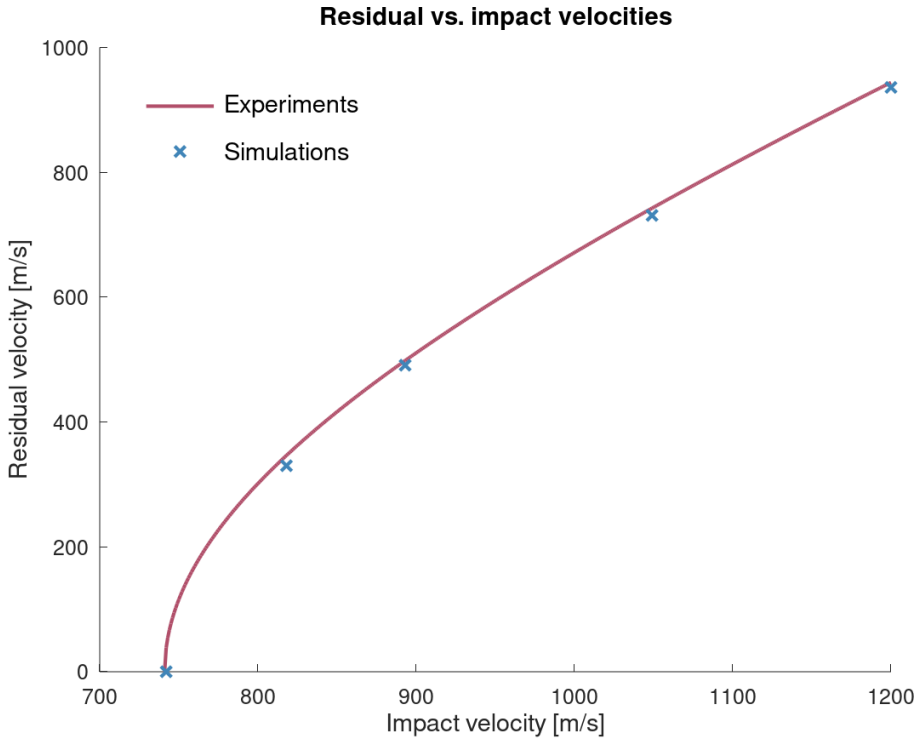

Figure 42: Residual velocities from the simulations and experiments with Hardox 400.

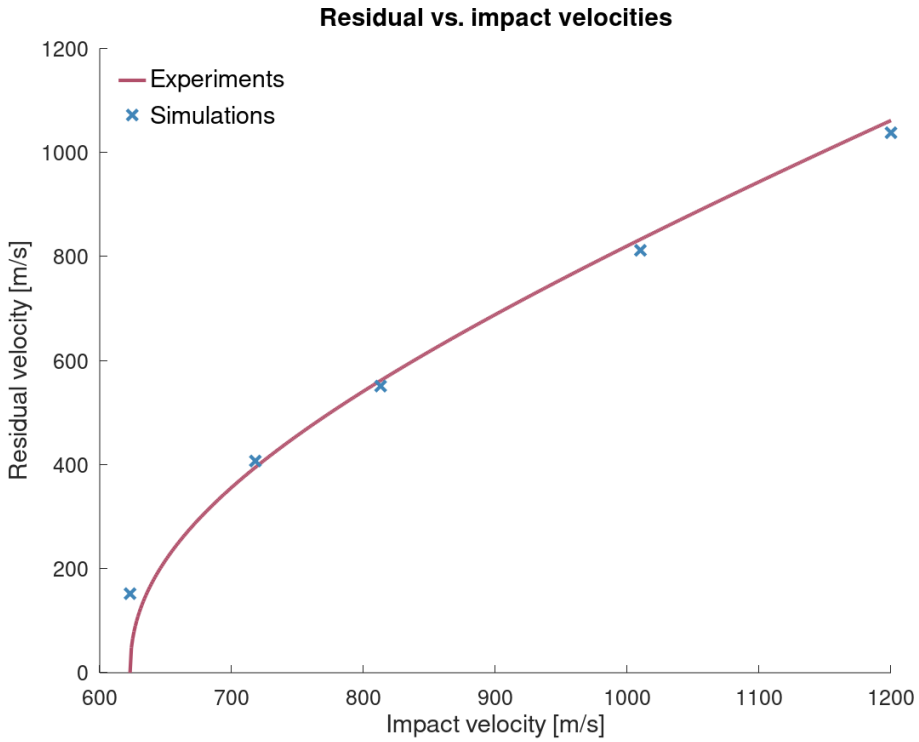

Figure 43: Residual velocities from the simulations and experiments with Weldox 500E.

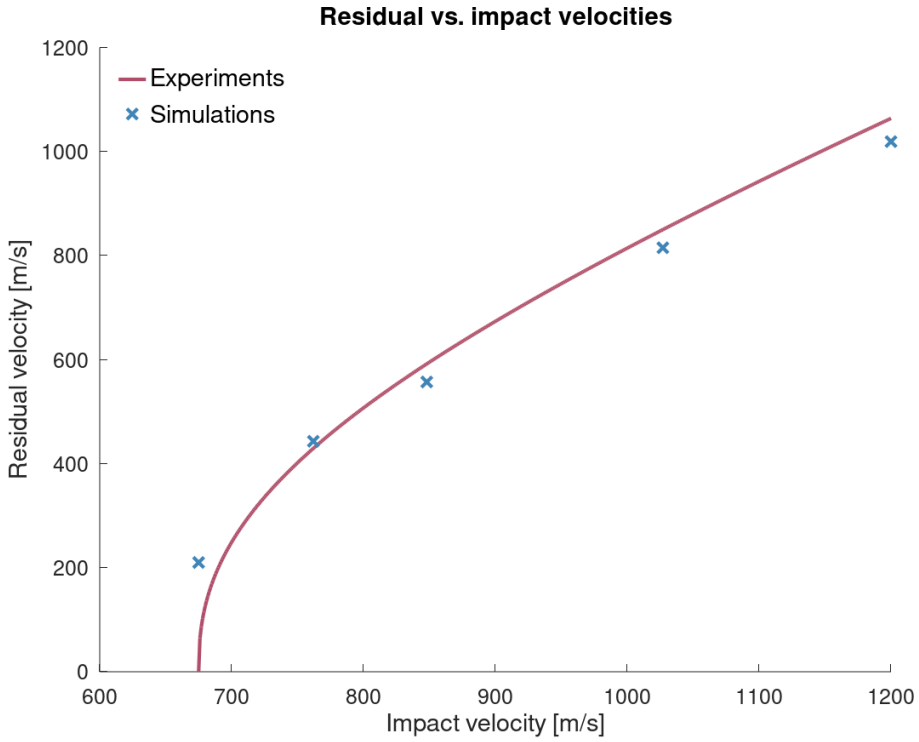

Figure 44: Residual velocities from the simulations and experiments with Weldox 700E.

One simulation of each material is subjected to version control.

References

1 - T. Børvik, S. Dey, A.H. Clausen, Perforation resistance of five different high-strength steel plates subjected to small-arms projectiles, International Journal of Impact Engineering, Volume 36, 2009, Pages 948-964.

Tests

This benchmark is associated with 4 tests.

T. Børvik et al. (2011)

Normal and oblique impact of small arms bullets on AA6082-T4 aluminium protective plates

Ballistic tests with target plates of AA6082-T4 impacted by 7.62 mm APM2 projectiles at different obliquity are presented in T. Børvik et al. (2011) [1]. A numerical model of the experiments is created to assess the calibrations of AA6082-T4 available in this material object.

Target plates with dimensions 300 x 300 x 20 mm are fixed with two opposite edges in a rotatable rig. The three calibrations of AA6082-T4 are used in the target plate to investigate the effects of anisotropy. The 7.62 mm APM2 projectile core is modeled as rigid, while models of brass and lead, which are used in the jacket and tip, are modeled in accordance to the referenced literature.

Investigated angles of obliquity are 0, 15, 30, 45 and 60°. The impact velocity was 830 $\pm$ 20 m/s in all cases and five to six tests were done for each obliquity. Residual velocities were registered in cases resulting in compete penetration.

Model settings:

- In-plane dimensions of the target plates are reduced to 50 - 135 x 50 mm in the model, depending on obliquity investigated.
- The edges of the target plate are fixed in the model.
- Third order hexahedrons are used exclusively.
- Cubic elements with a side length of 1.0 mm are used in the impact zone.
- Half symmetry is utilized as visible in Figure 45.
- A deviatoric erosion strain of 3.0 (300%) is used to maintain a reasonable time step size.
- A friction coefficient of 0.02 (2%) is assumed.

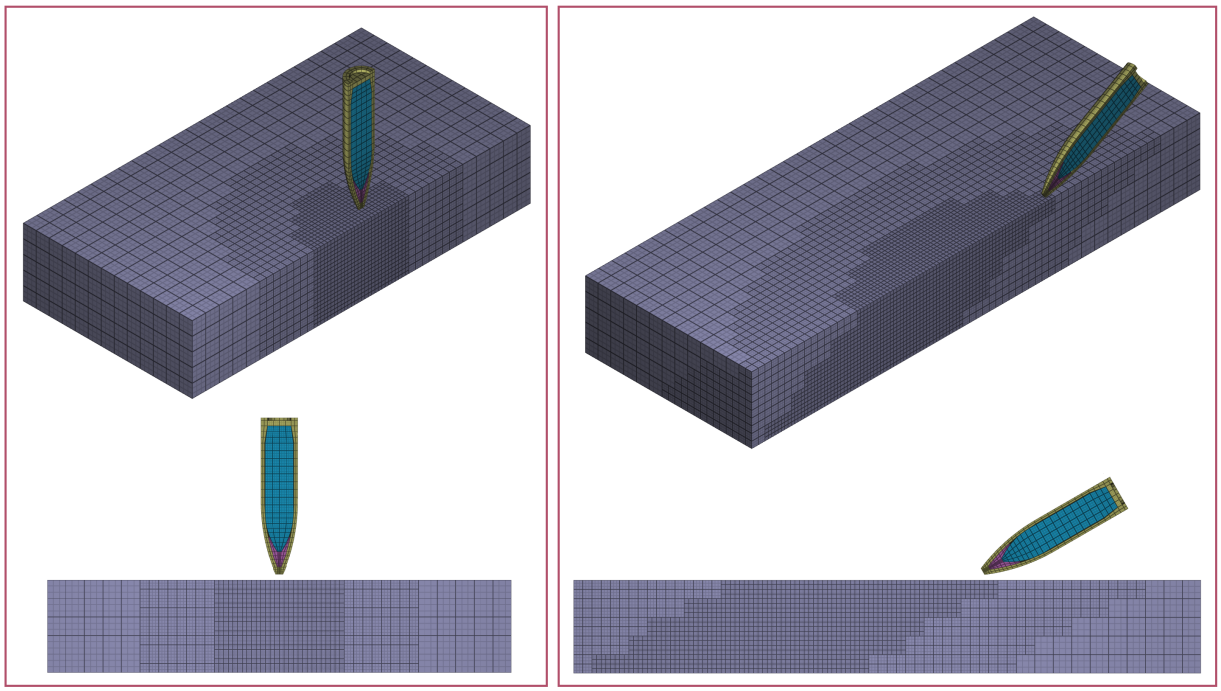

Figure 45: Half symmetry models of target plate and the 7.62 mm APM2 projectile. The target plates are refined in the impact zone. To the left: normal impact (0° obliquity). To the right: impact at 60° obliquity

Residual velocities from the simulations are compared to a curve fitted to the residual velocities found from the experiments in Table 18 - 20 and Figure 46. The uncertainty of the curve increases with the obliquity since the spread in experimental data increased with the angle of obliquity. Details regarding the curve are presented in the referenced literature.

Cross-sectional views of the target plates from simulations with the 0°-calibration are compared to photos from the experiment in Figure 47.

Table 18: Residual velocities from experiments, $v_{r,exp}$, and simulations, $v_{r,sim}$, at different obliquity. Simulations are with the 0°-calibration of AA6082-T4.

Obliquity [°]	$\mathbf{v_{r,exp}}$ $[m/s]$	$\mathbf{v_{r,sim}}$ $[m/s]$	**Error** [%]
0	720	719	-0.1
15	720	708	-1.7
30	709	679	-4.2
45	592	595	0.5
60	0	0	0.0

Table 19: Residual velocities from experiments, $v_{r,exp}$, and simulations, $v_{r,sim}$, at different obliquity. Simulations are with the 45°-calibration of AA6082-T4.

Obliquity [°]	$\mathbf{v_{r,exp}}$ $[m/s]$	$\mathbf{v_{r,sim}}$ $[m/s]$	**Error** [%]
0	720	731	1.5
15	720	724	0.6
30	709	698	-1.6
45	592	636	7.4
60	0	0	0.0

Table 20: Residual velocities from experiments, $v_{r,exp}$, and simulations, $v_{r,sim}$, at different obliquity. Simulations are with the 90°-calibration of AA6082-T4.

Obliquity [°]	$\mathbf{v_{r,exp}}$ $[m/s]$	$\mathbf{v_{r,sim}}$ $[m/s]$	**Error** [%]
0	720	726	0.8
15	720	718	-0.3
30	709	697	-1.7
45	592	621	4.9
60	0	0	0.0

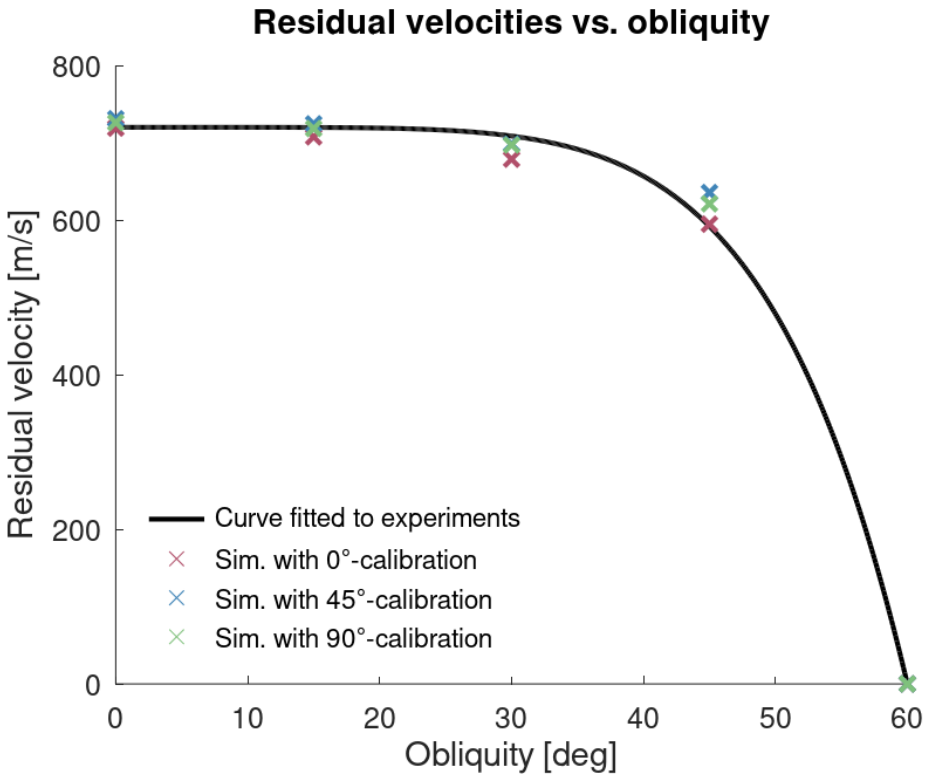

Figure 46: Residual velocities from experiments and simulations at different obliquity.

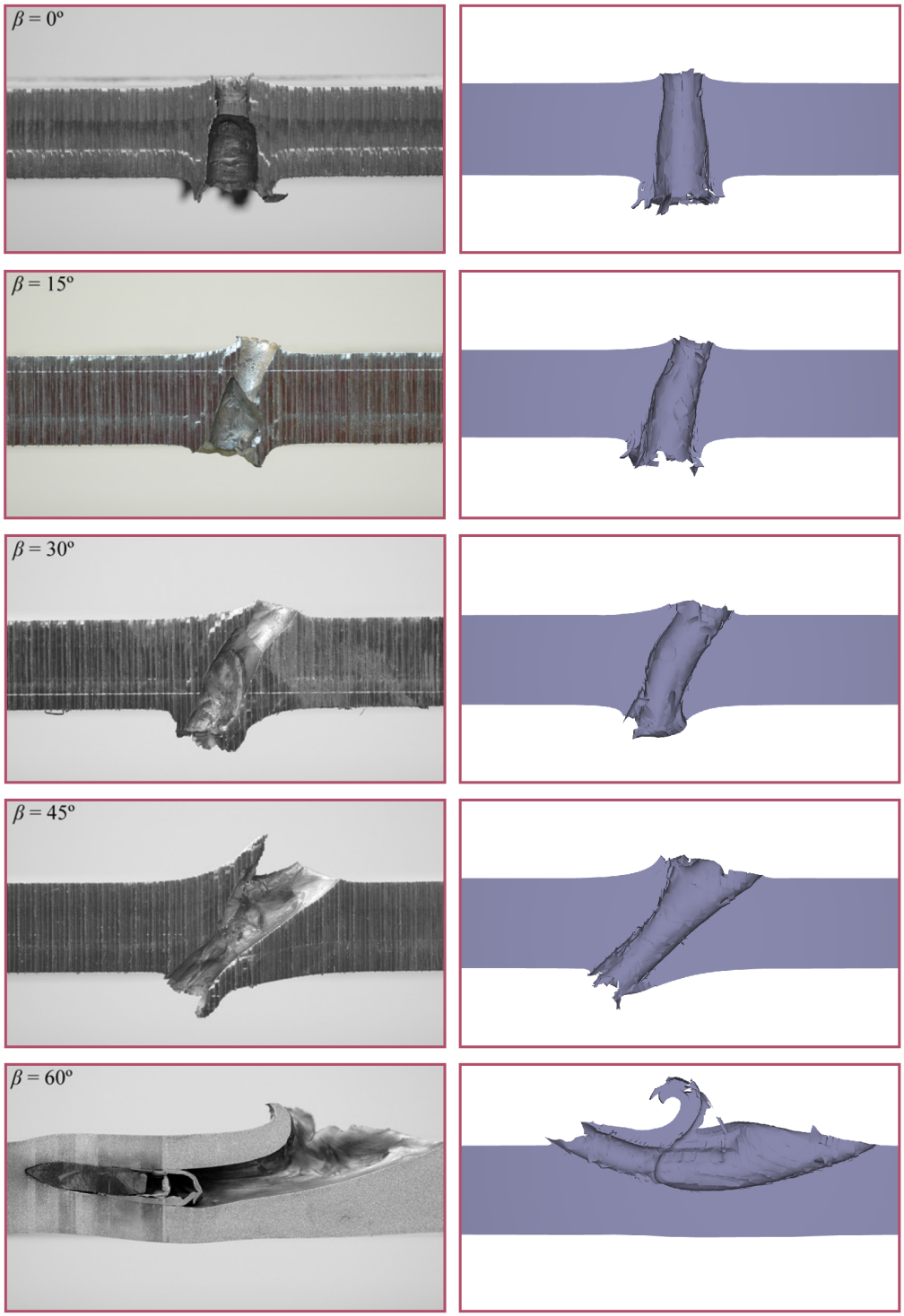

Figure 47: Cross-sectional view of the target plates from experiments and simulations. Obliquity from top to bottom: 0, 15, 30, 45 and 60°.

In the experiments, the projectile gets embedded in the target plate at 60° obliquity while ricochet is observed in the simulation. An additional simulation was run with an obliquity of 58° and a better resemblance to the experiment is achieved, as visible in Figure 48.

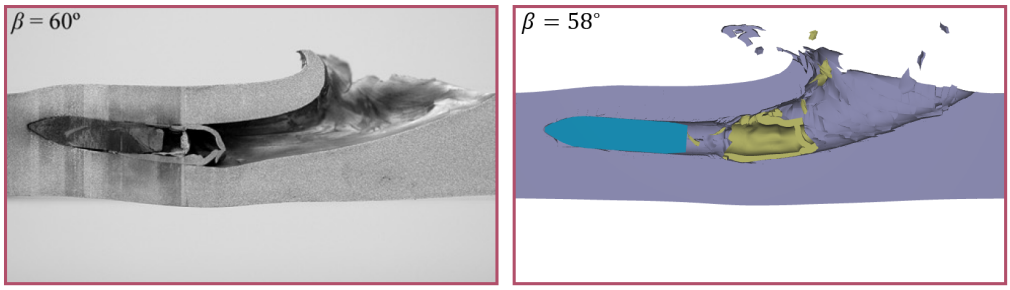

Figure 48: A better resemblance to the experiment was achieved by reducing the obliquity to 58° in the simulation.

The simulations with 30° obliquity are subjected to version control.

References

1 - T. Børvik, L. Olovsson, S. Dey, M. Langseth, Normal and oblique impact of small arms bullets on AA6082-T4 aluminium protective plates, International Journal of Impact Engineering, Volume 38, 2011, Pages 577-589.

Tests

This benchmark is associated with 12 tests.

CONTACT NORWAY: IMPETUS Afea AS
Strandgaten 32, 4400 Flekkefjord, Norway
Phone: + 47 95 72 58 01

CONTACT SWEDEN: IMPETUS Afea AB
Huddinge Stationsväg 7B, SE-14135 Huddinge, Sweden
Phone: + 46 70 184 98 73

sales@impetus.no
https://www.impetus.no